

PENELOPE (v. 2006)

A coupled electron-photon transport code

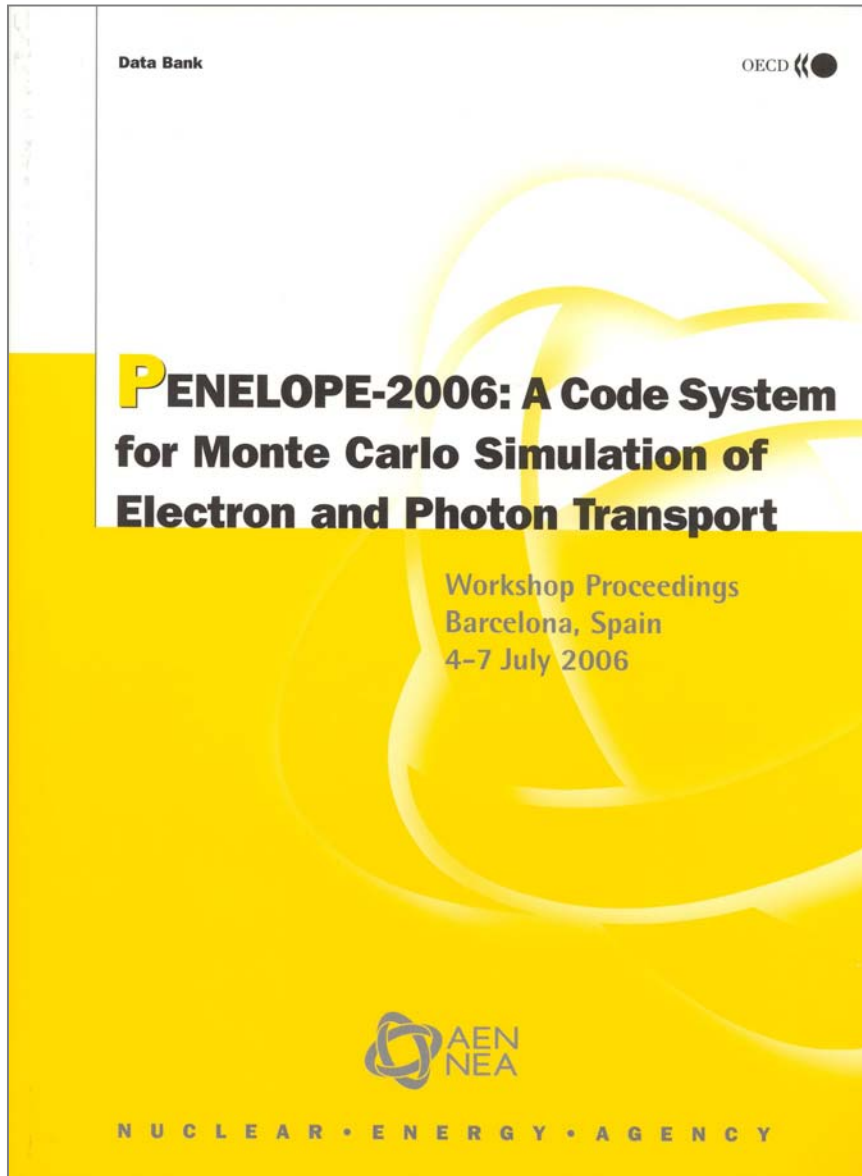
Francesc Salvat,
José M Fernández-Varea, Josep Sempau,
Xavier Llovet, David Bote



□ Outline

- PENELOPE
- Photon interactions and transport
- Electron interactions
- Electron transport
- Constructive quadric geometry
- Some applications

□ PENELOPE



PENetration and **E**nergy **L**Oss of **P**ositrons and **E**lectrons... and photons

F Salvat, JM Fernández-Varea, J Sempau

A general-purpose Monte Carlo code

Distributed by the OECD-NEA Data Bank, Paris (~600 registered users)

<http://www.nea.fr/lists/penelope.html>

Available also from RSICC,
and from the authors

❑ Main features

- ❑ All kinds of interactions (except nuclear reactions) in the energy range
from ~ 50 eV to 10^9 eV
(covered by the database)
- ❑ Implements the most accurate physical models available (limited only by the required generality)
- ❑ Simulates electrons and positrons (tunable mixed scheme) **and** photons (detailed, interaction by interaction)
- ❑ Simulates fluorescent radiation from K, L and M shells
- ❑ Includes a flexible geometry package (constructive quadric geometry)
- ❑ Electron and positron transport in **external** magnetic and electric fields (in matter)

❑ Specific features

All Monte Carlo codes, including PENELOPE, are plagued with approximations, both in the physical interaction models and in the electron transport algorithms

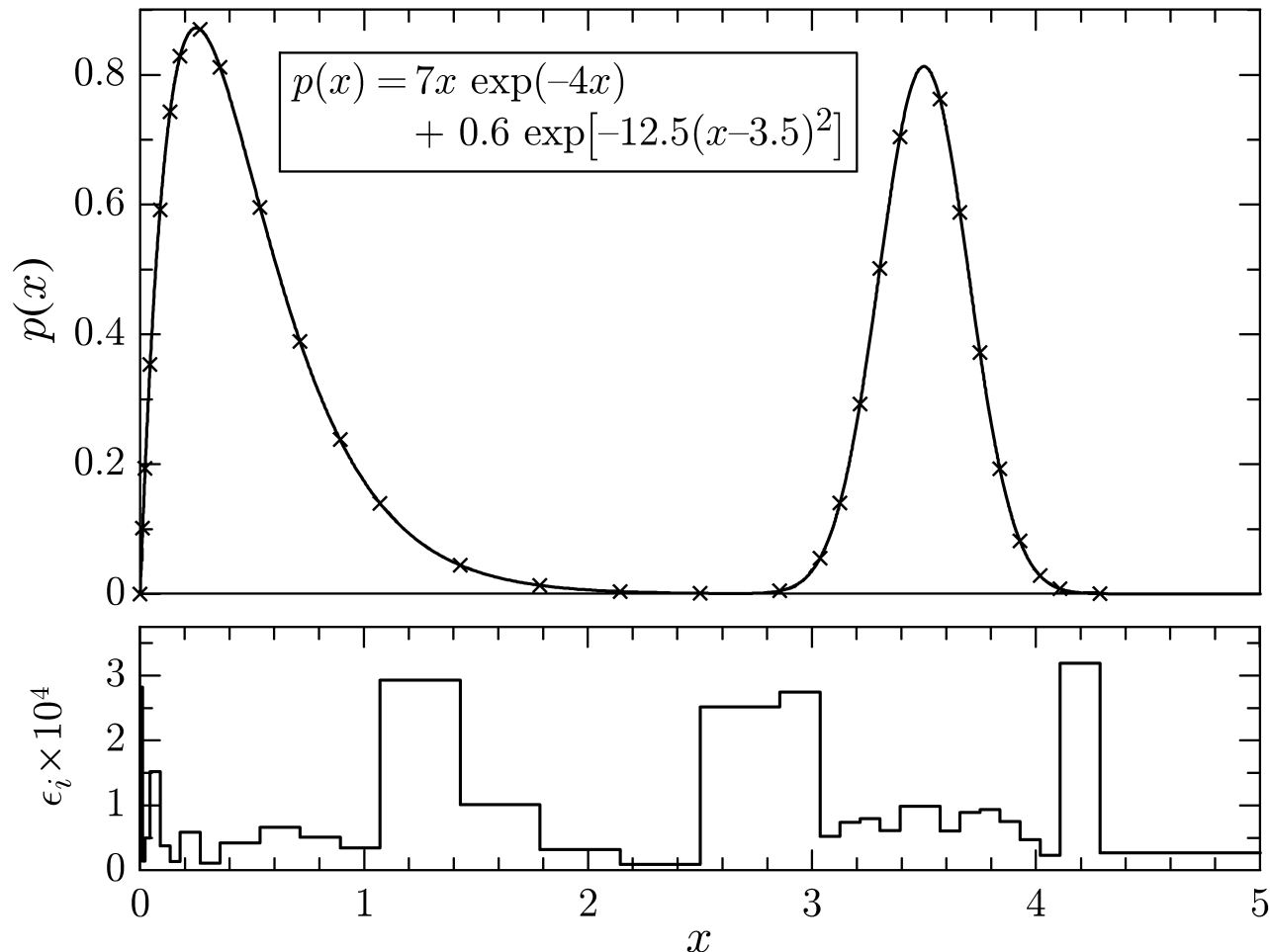
- ❑ PENELOPE evolved from low-energy (keV) electron-transport MC codes, which were used in the late 1980s to simulate electron microscopy and conversion-electron Mössbauer spectroscopy.
 - ⇒ The main difference is in the electron transport mechanics
- ❑ Our main research is in theoretical atomic physics. We develop models and codes for calculating interaction cross sections. When a model is proven to be robust and general, we generate an extensive database and plug it into PENELOPE, replacing older models.
 - ⇒ PENELOPE is evolving continuously. Specificities of different materials
- ❑ PENELOPE is structured as a subroutine package (in the style of most codes used in atomic and nuclear physics).
 - ⇒ The user has complete access to the physical parameters...
 - ⇒ Example main programs are provided (PENSLAB, PENCYL, PENMAIN)

□ Random sampling (RITA method)

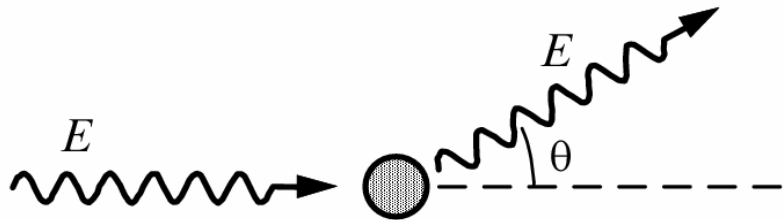
Piecewise Rational Inverse Transform with Aliasing. Adaptive, very accurate

$$\tilde{\mathcal{P}}^{-1}(\xi) = x_i + \frac{(1 + a_i + b_i)\eta}{1 + a_i\eta + b_i\eta^2} (x_{i+1} - x_i); \quad \eta = \frac{\xi - \xi_i}{\xi_{i+1} - \xi_i}, \quad \text{if } \xi_i \leq \xi < \xi_{i+1}$$

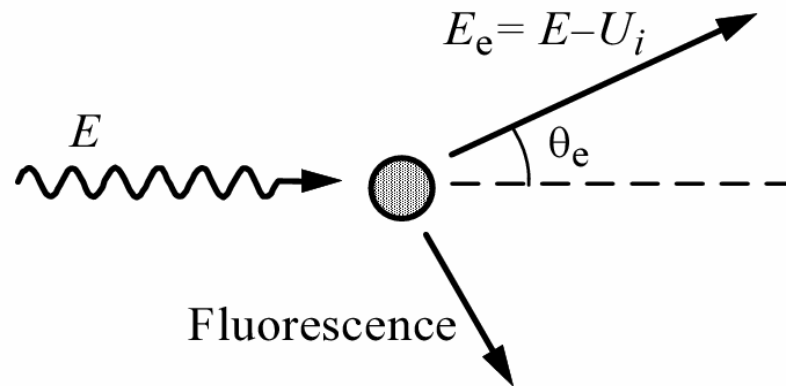
32 points:



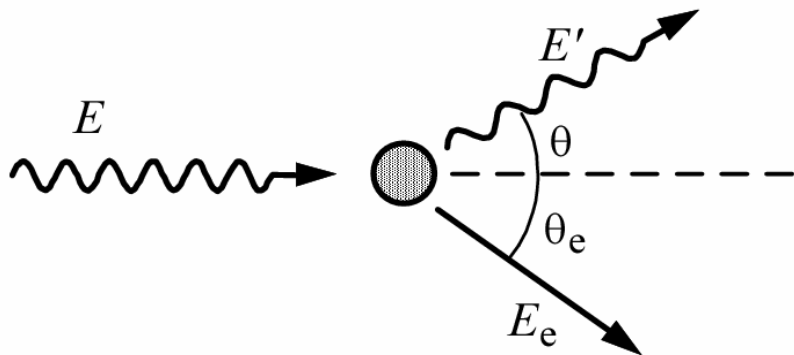
□ Photon interactions



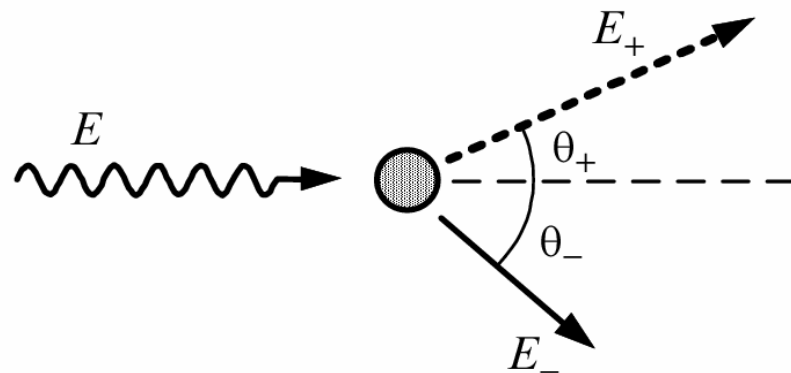
Rayleigh scattering



Photoelectric absorption



Compton scattering



Pair production

□ Rayleigh (coherent) scattering

□ Thompson scattering

Elastic scattering by free electrons at rest (non-relativistic)

$$\frac{d\sigma_T}{d\Omega} = r_e^2 \frac{1 + \cos^2 \theta}{2}$$

θ = polar scattering angle

$r_e \equiv e^2 / (m_e c^2) \simeq 2.8 \text{ fm}$ is the classical electron radius

□ Rayleigh scattering

Elastic scattering by neutral atoms. Born (form factor) approximation

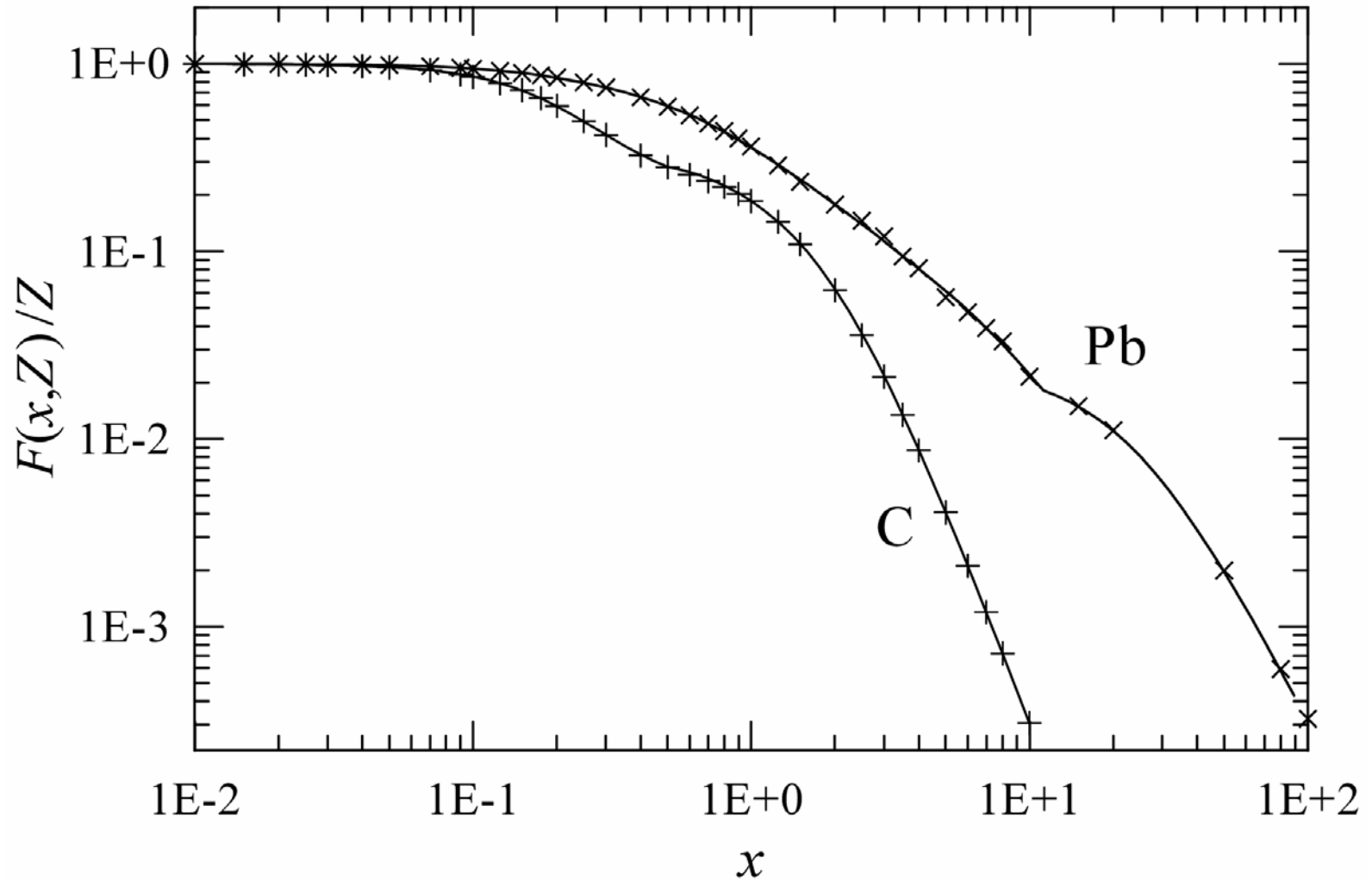
$$\frac{d\sigma_{Ra}}{d\Omega} = \frac{d\sigma_T}{d\Omega} [F(q, Z)]^2$$

q = momentum transfer

$$q = 2(E/c) \sin(\theta/2) = (E/c) [2(1 - \cos \theta)]^{1/2}$$

$F(q, Z)$ = atomic form factor... $x = 20.6 \frac{q}{m_e c}$

Atomic form factors



Tables of Hubbell et al. (1975), EPDL

Continuous curves: Analytical approximation (Baró et al, 1994)

□ Photoelectric effect

□ LLNL's EPDL '97 database (Cullen et al., 1997)

□ Scofield's calculation of $\sigma_{\text{ph},i}(E)$ $i = \text{K, L1-L3, M1-M5 shells}$

- independent-electron model: Dirac-Hartree-Fock-Slater
- 1st-order perturbation theory
- matrix elements $\langle \psi_f | e \boldsymbol{\alpha} \cdot \mathbf{A} | \psi_i \rangle$

□ Hubbell's compilation of $\sigma_{\text{ph}}(E)$

Large uncertainties below ~ 1 keV

□ Initial direction of photoelectrons.

Sauter relativistic DCS for ionization of hydrogenic ions
(approximately valid for K-shell electrons).

Compton (incoherent) scattering

- Elementary models: Klein-Nishina (free electrons at rest),
Waller-Hartree (bound electrons at rest)

Relativistic impulse approximation.

Provides a consistent description of

- Binding effects (target electrons are bound)
- Doppler broadening (target electrons “move”)

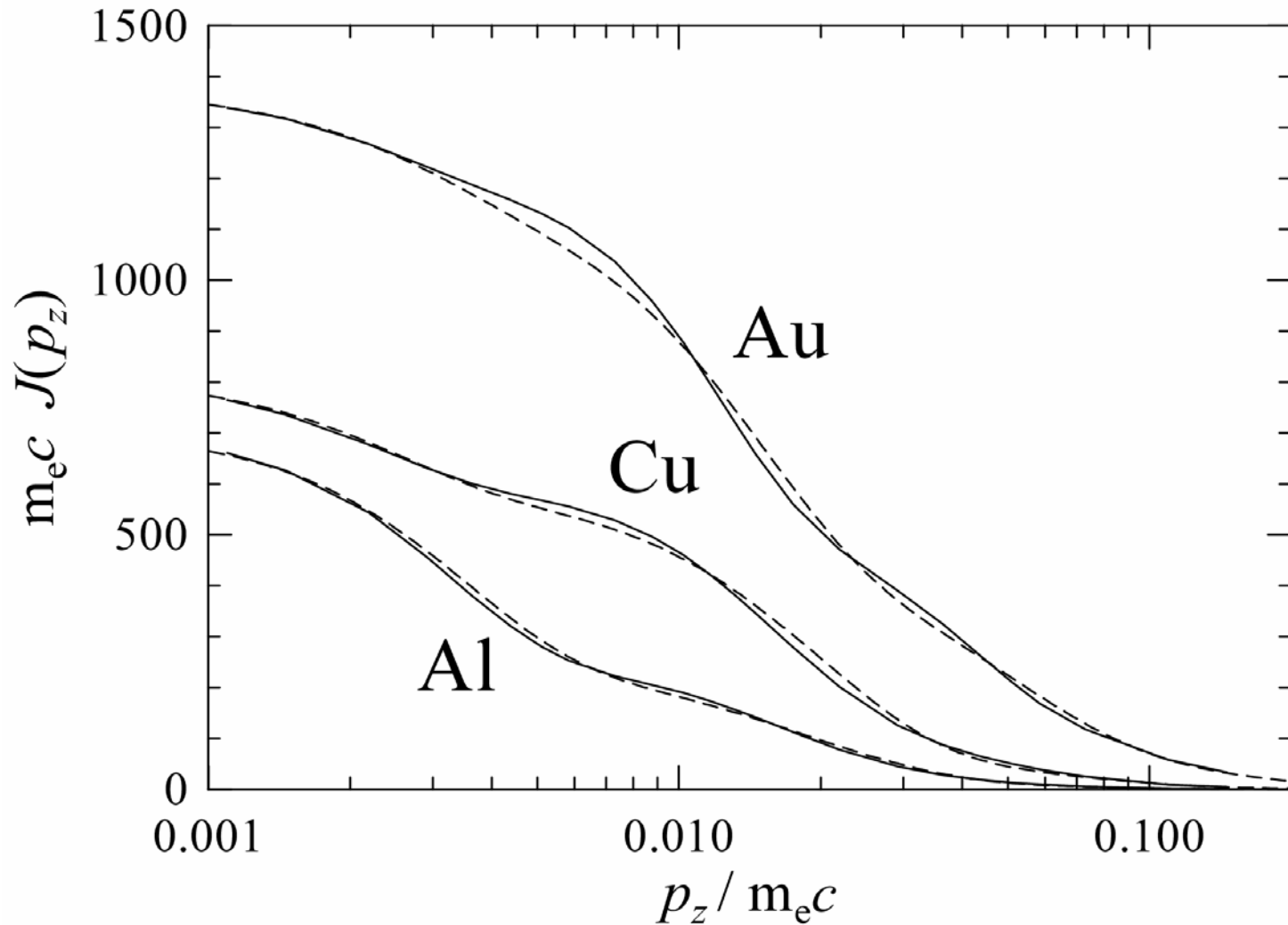
$$\frac{d^2\sigma_{\text{Co}}}{dE' d\Omega} = \frac{r_e^2}{2} \left(\frac{E_C}{E}\right)^2 \left(\frac{E_C}{E} + \frac{E}{E_C} - \sin^2\theta\right) \times F(p_z) \left(\sum_i f_i J_i(p_z) \Theta(E - E' - U_i)\right) \frac{dp_z}{dE'}$$

where

$$q \equiv |\hbar\mathbf{k} - \hbar\mathbf{k}'| = \frac{1}{c} \sqrt{E^2 + E'^2 - 2EE' \cos\theta}$$
$$p_z \equiv -\mathbf{p} \cdot \mathbf{q} / q \qquad E_C \equiv \frac{E}{1 + \frac{E}{m_e c^2} (1 - \cos\theta)}$$

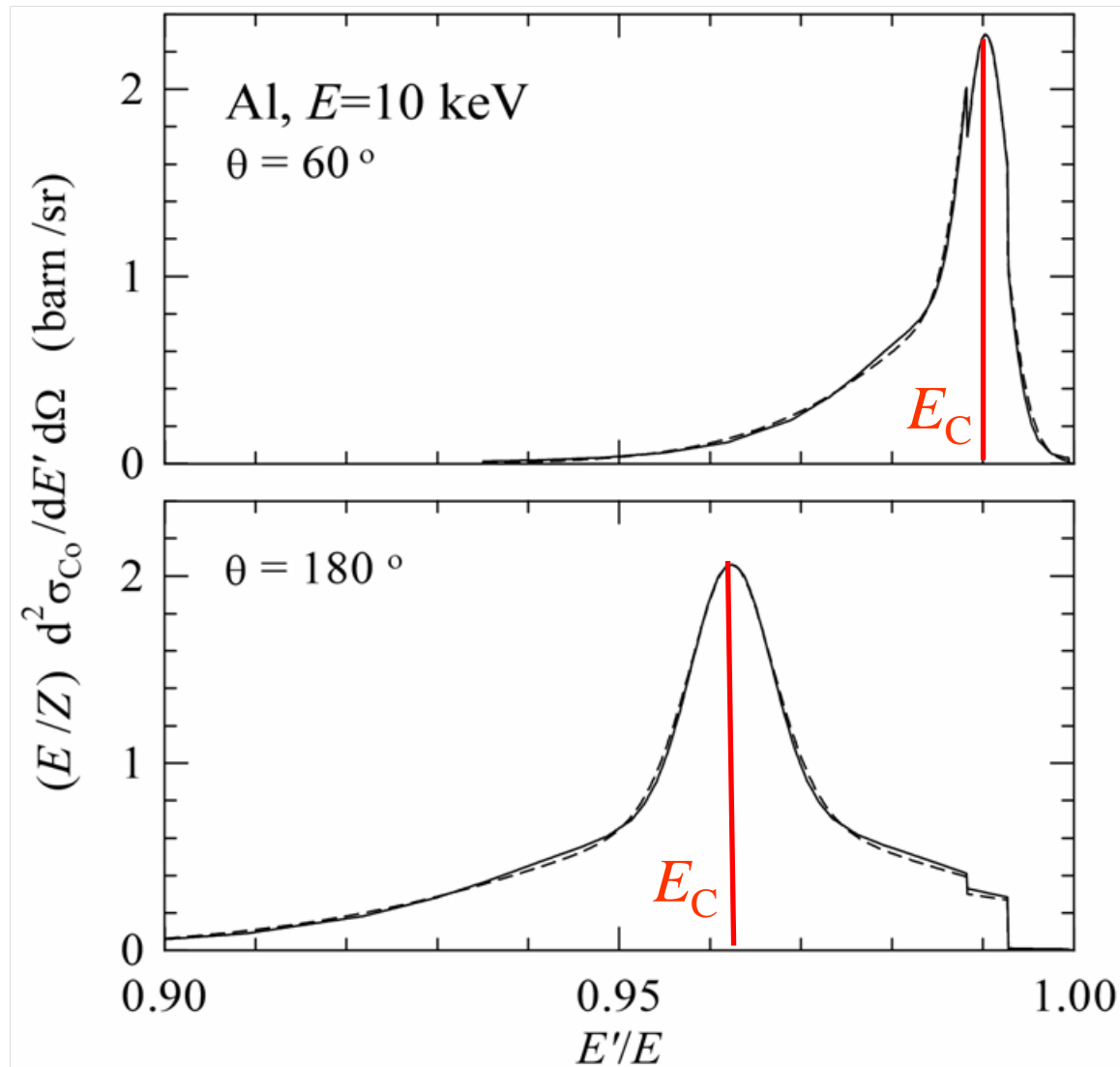
$J_i(p_z)$ = Compton profile of shell $i=(n, j, \ell)$ with f_i electrons and binding energy U_i

Atomic Compton profiles



Continuous curves: numerical HF profiles (Biggs et al., 1975).
Dashed curves: analytical profiles.

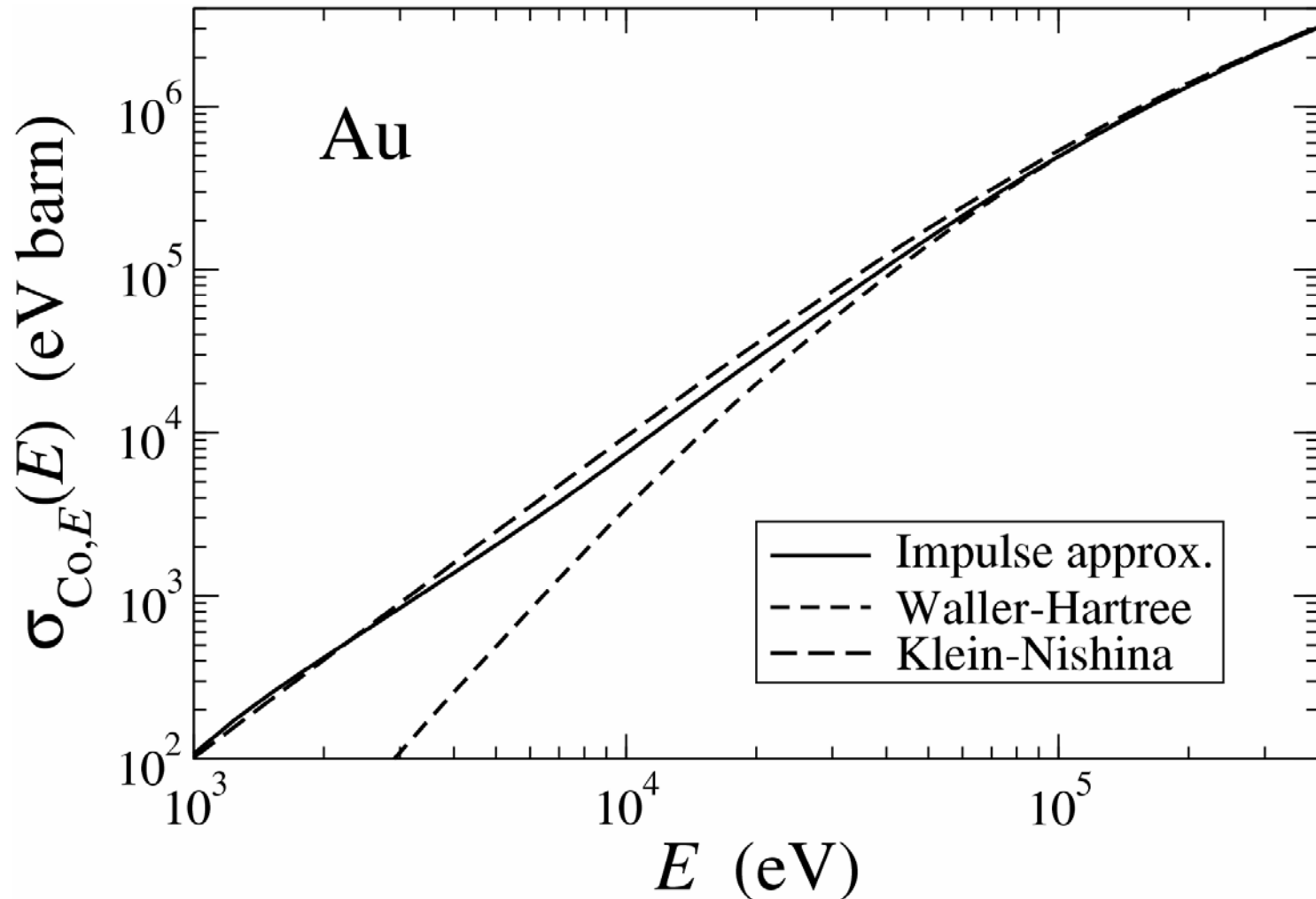
□ Double DCS for 10 keV photons in Al



Continuous curves: calculated with numerical HF profiles.
Dashed curves: calculated with the analytical profiles.

□ Energy-deposition cross section

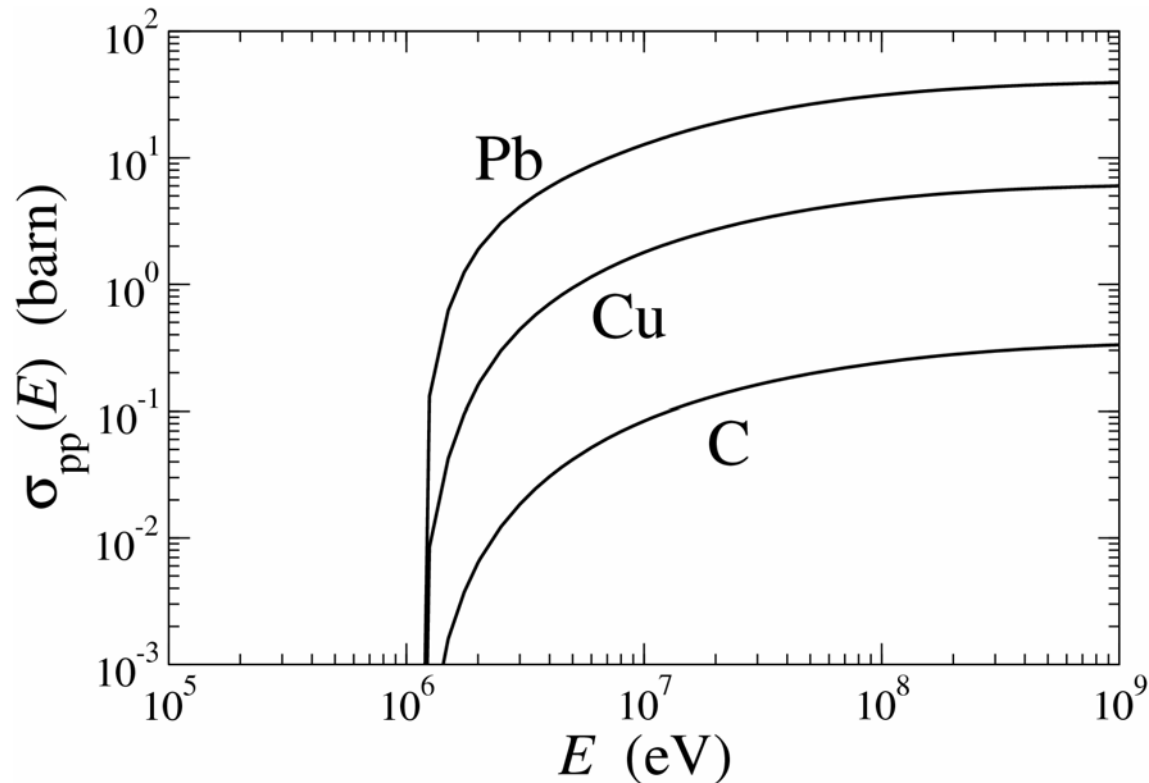
$$\sigma_{\text{Co},E} = \int_0^E (E - E') \frac{d\sigma_{\text{Co}}}{dE'} dE'$$



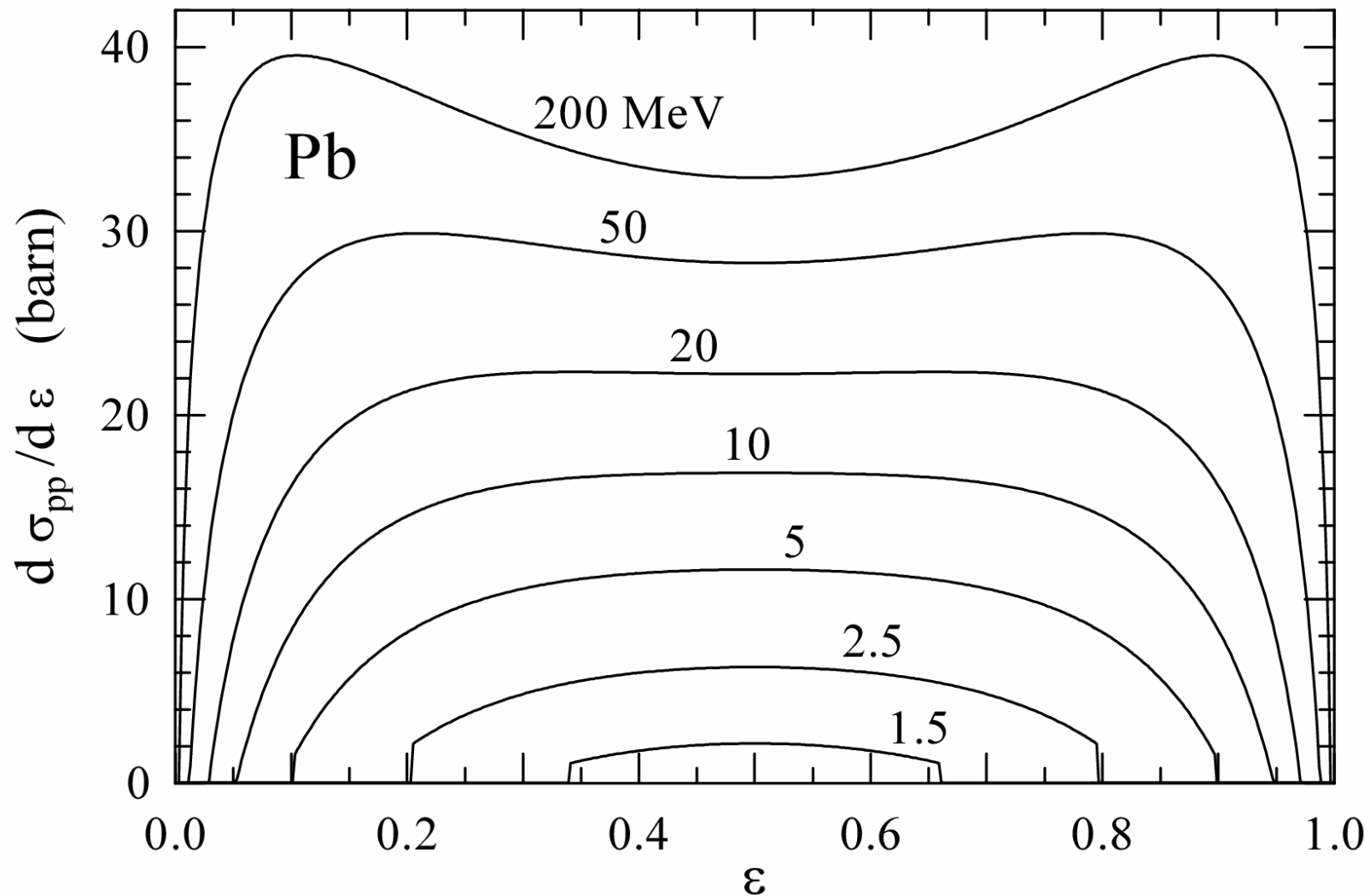
□ Electron-positron pair production

□ Bethe-Heitler DCS

- Born approximation with exponential screening
- High-energy Coulomb correction
- Empirical (fitted) low-energy correction
- Attenuation coefficient from EPDL (pair + triplet)

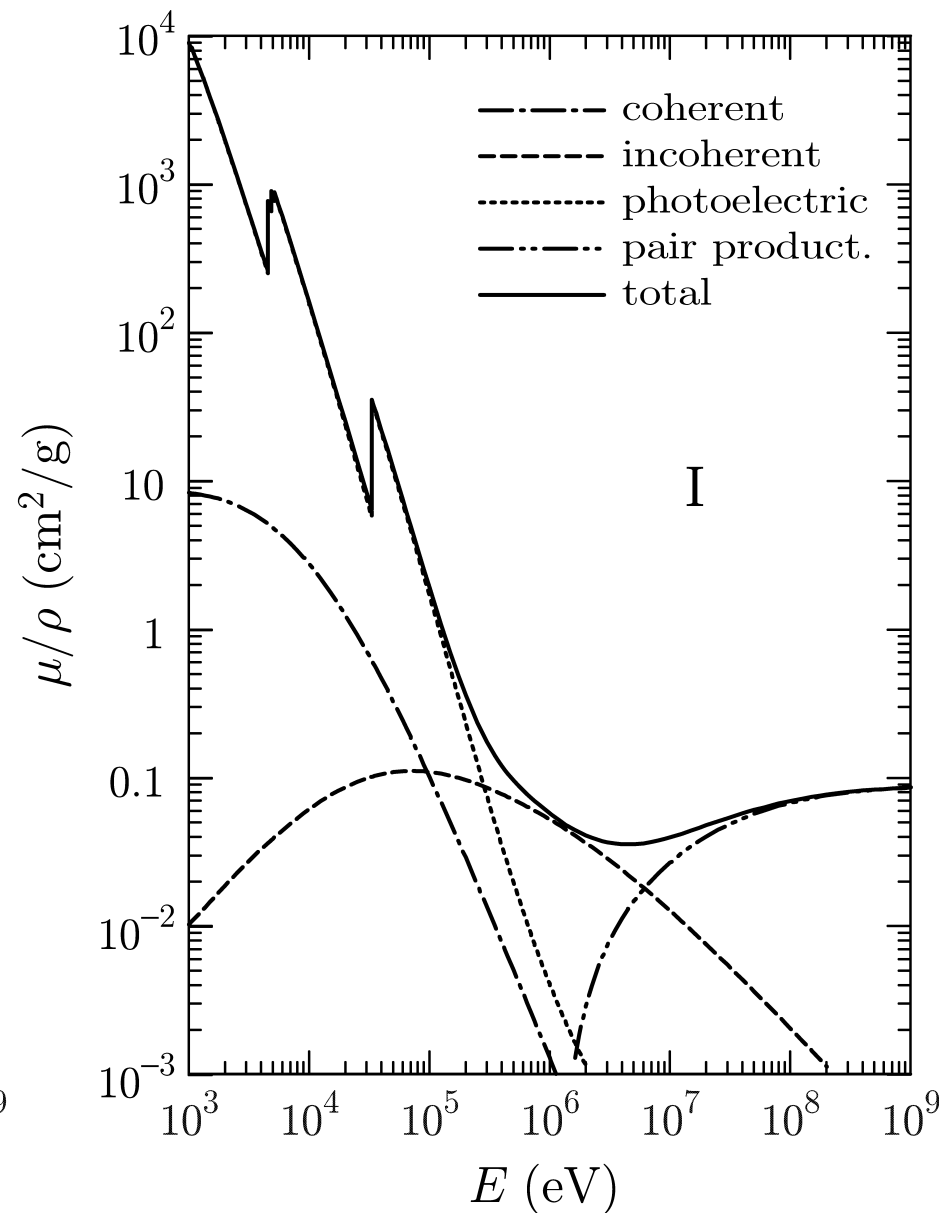
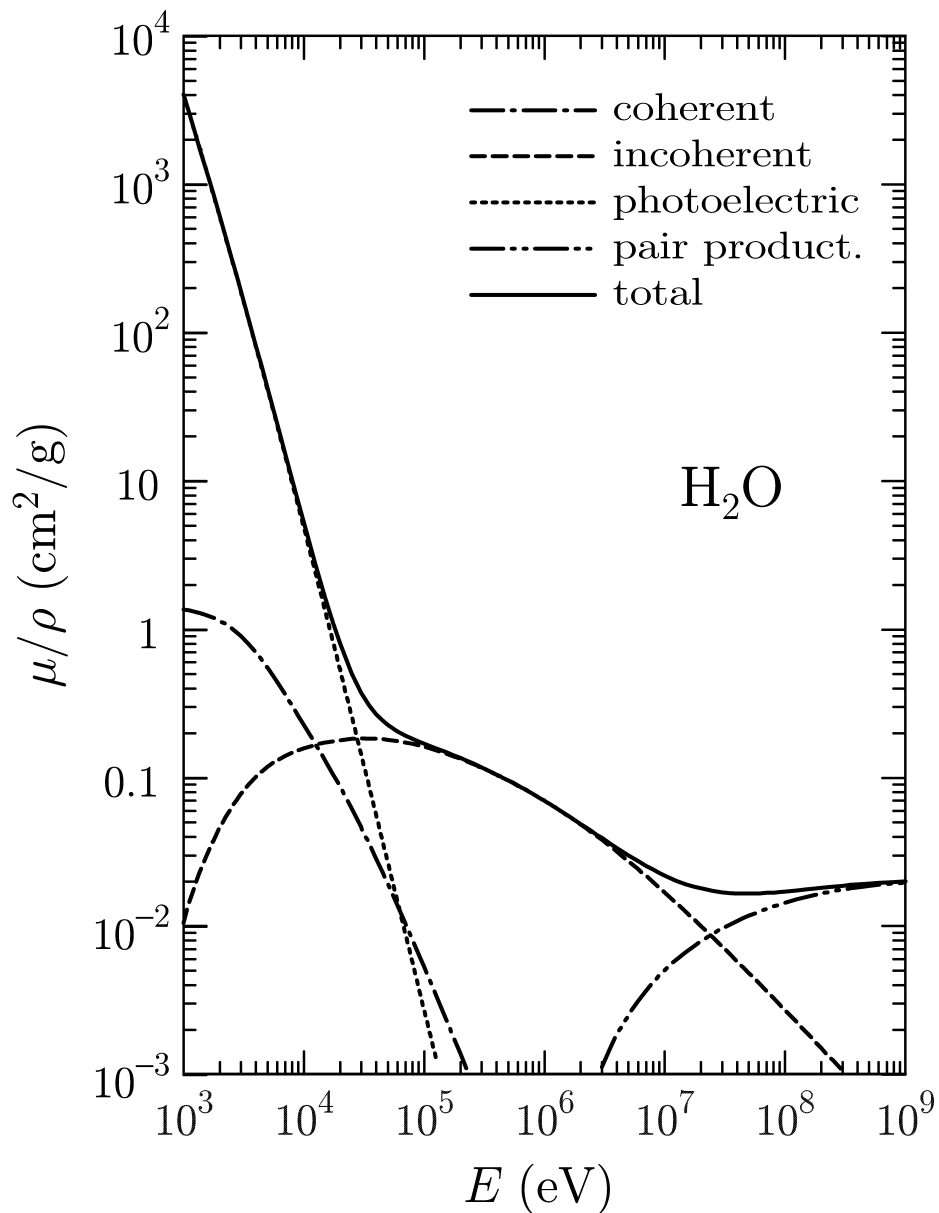


Pair-production DCS of Pb

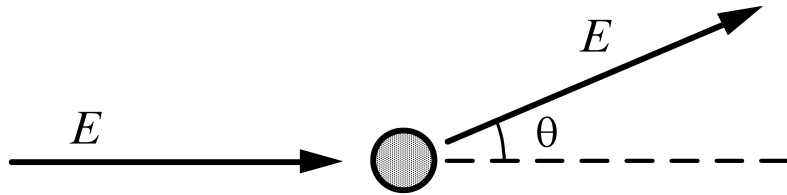


WARNING: the DCS should be asymmetrical near the pp threshold

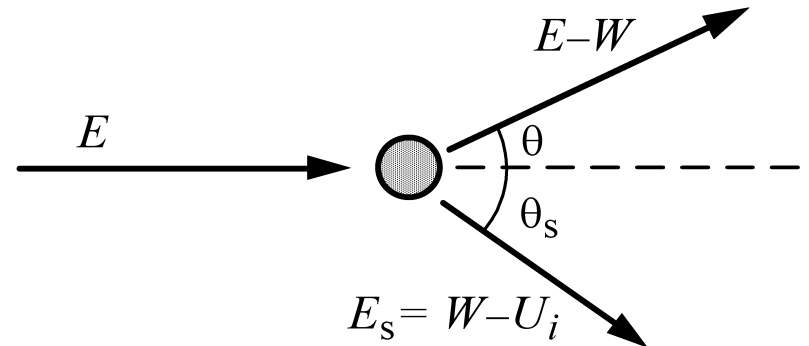
Partial and total mass-attenuation coefficients



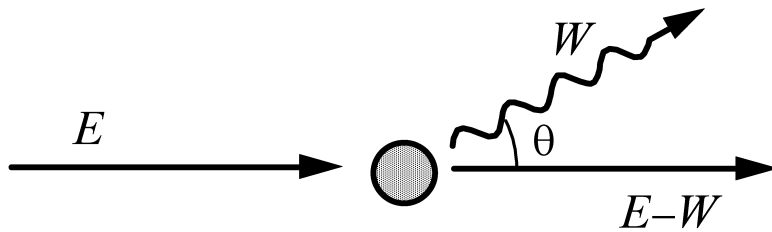
Interactions of electrons and positrons



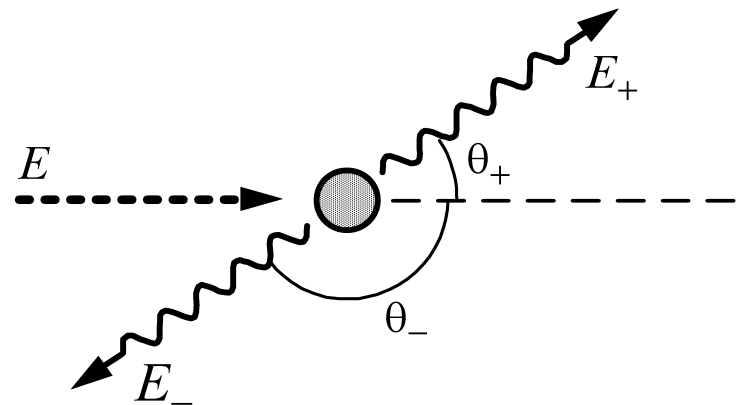
Elastic scattering



Inelastic scattering



Bremsstrahlung emission



Positron annihilation

□ Elastic collisions

Collisions without electronic excitation of the target.

Because of the smallness of the electron mass ($\ll M_{\text{nuc}} \approx 3600 Z m_e$) recoil energy losses are negligible.

Static-field approximation: Potential scattering theory

$V(r)$ = electrostatic interaction (+ local exchange for e^-)

Polar angular deflection: θ , scattering angle or $\mu \equiv \frac{1 - \cos \theta}{2}$

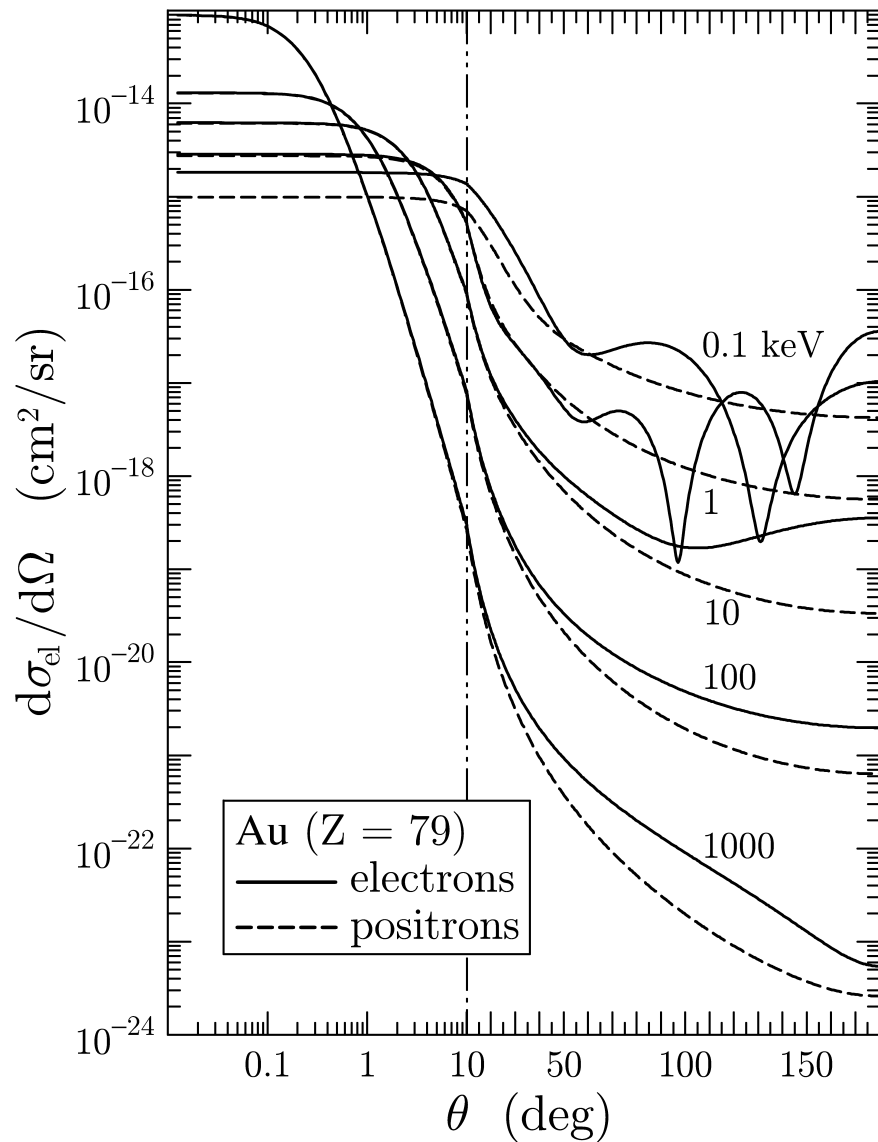
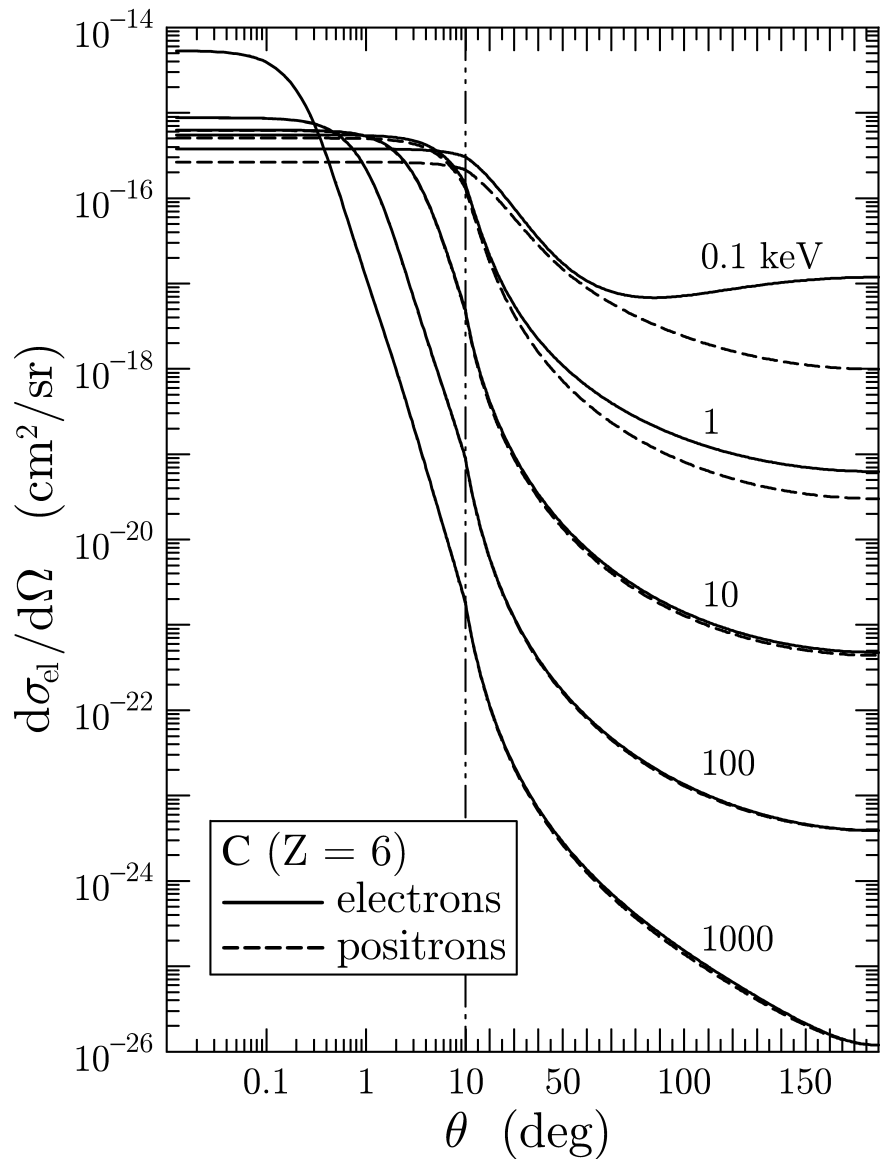
Relativistic (Dirac) partial-wave analysis:

$$\frac{d\sigma_{\text{el}}}{d\Omega} = |f(\theta)|^2 + |g(\theta)|^2$$

$$f(\theta) = \frac{1}{2ik} \sum_{\ell=0}^{\infty} \{(\ell + 1) [\exp(2i\delta_{-\ell-1}) - 1] + \ell [\exp(2i\delta_{\ell}) - 1]\} P_{\ell}(\cos \theta)$$

$$g(\theta) = \frac{1}{2ik} \sum_{\ell=0}^{\infty} [\exp(2i\delta_{\ell}) - \exp(2i\delta_{-\ell-1})] P_{\ell}^1(\cos \theta)$$

□ Numerical Database: ICRU 77, NIST, CPC (ELSEPA)



□ Integrated cross sections

Total cross section $\sigma_{\text{el}} = \int \frac{d\sigma_{\text{el}}}{d\Omega} d\Omega = \int_0^\pi \frac{d\sigma_{\text{el}}}{d\Omega} 2\pi \sin \theta d\theta$

Elastic mean free path $\lambda_{\text{el}} = \frac{1}{\mathcal{N}\sigma_{\text{el}}}$

Transport cross sections $\sigma_{\text{el},\ell} = \int [1 - P_\ell(\cos \theta)] \frac{d\sigma_{\text{el}}}{d\Omega} d\Omega$

Transport mean free paths $\lambda_{\text{el},\ell} = \frac{1}{\mathcal{N}\sigma_{\text{el},\ell}}$

$$\lambda_{\text{el},1}^{-1} = \frac{2\langle\mu\rangle}{\lambda_{\text{el}}} = \text{average angular deflection per unit path length (scattering power)}$$

$$\lambda_{\text{el},2}^{-1} = \frac{6(\langle\mu\rangle - \langle\mu^2\rangle)}{\lambda_{\text{el}}}$$

□ Inelastic collisions

Collisions that cause electronic excitation of the target.

□ Plane-wave first Born approximation

Double differential cross section (Fano, 1963)

$$\frac{d^2\sigma_{\text{in}}}{dW dQ} = \frac{2\pi e^4}{m_e v^2} \left(\frac{2m_e c^2}{W Q (Q + 2m_e c^2)} + \frac{\beta^2 \sin^2 \theta_r W 2m_e c^2}{[Q(Q + 2m_e c^2) - W^2]^2} \right) \frac{df(Q, W)}{dW}$$

longitudinal

transverse

W = energy loss, θ_r = recoil angle between \mathbf{p} and $\mathbf{q}=\mathbf{p}-\mathbf{p}'$

Q = recoil energy $Q(Q + 2m_e c^2) = (cq)^2 = c^2(p^2 + p'^2 - 2pp' \cos \theta)$

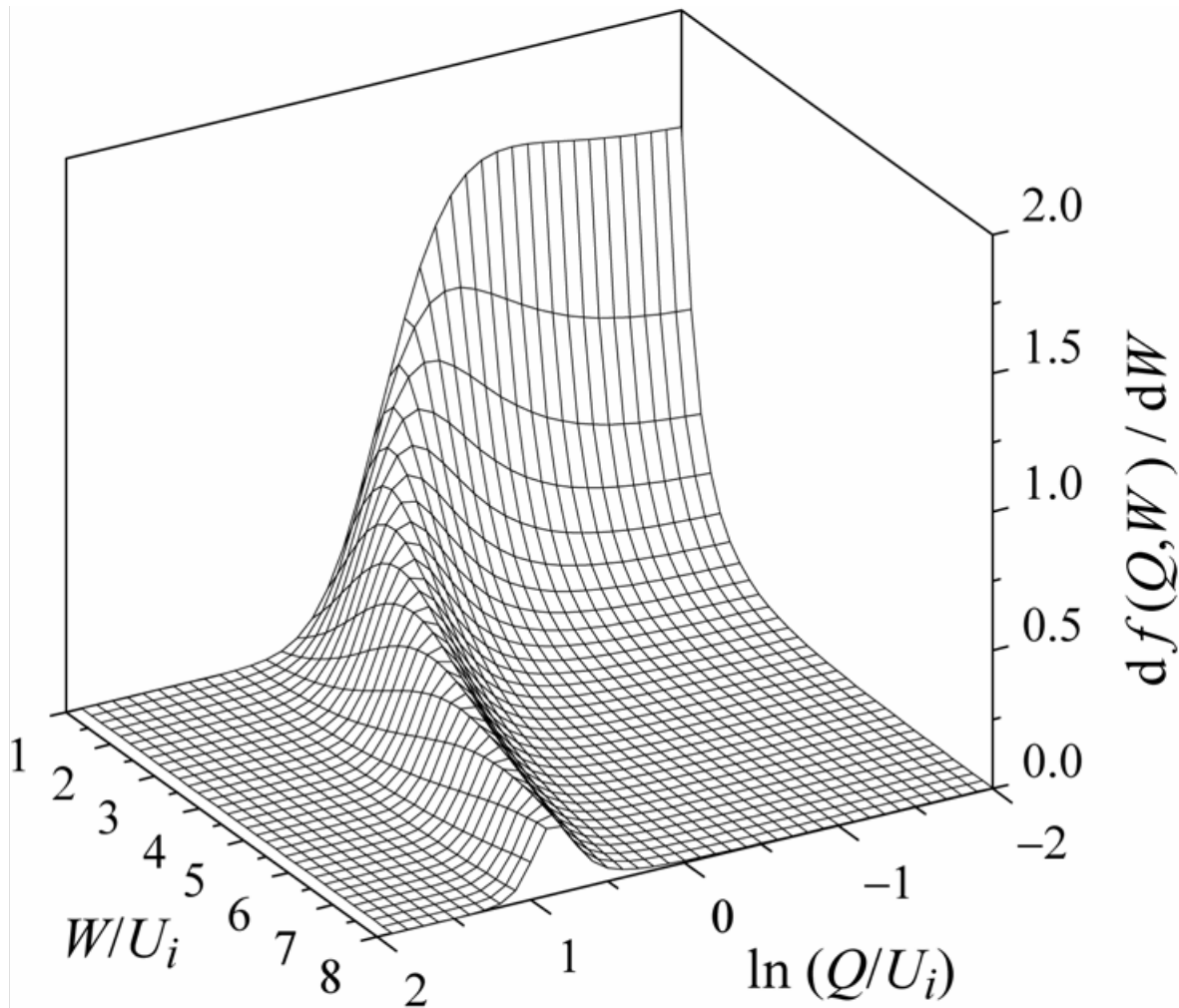
□ Generalized oscillator strength (GOS)

$$\frac{df(Q, W)}{dW} \equiv \frac{W}{Q} \left| \langle \Psi | \sum_{j=1}^Z \exp(i\mathbf{q} \cdot \mathbf{r}_j / \hbar) | \Psi_0 \rangle \right|^2$$

Independent-electron model.

❑ Bethe surface

GOS of the hydrogen atom ($U_i = 13.6$ eV)



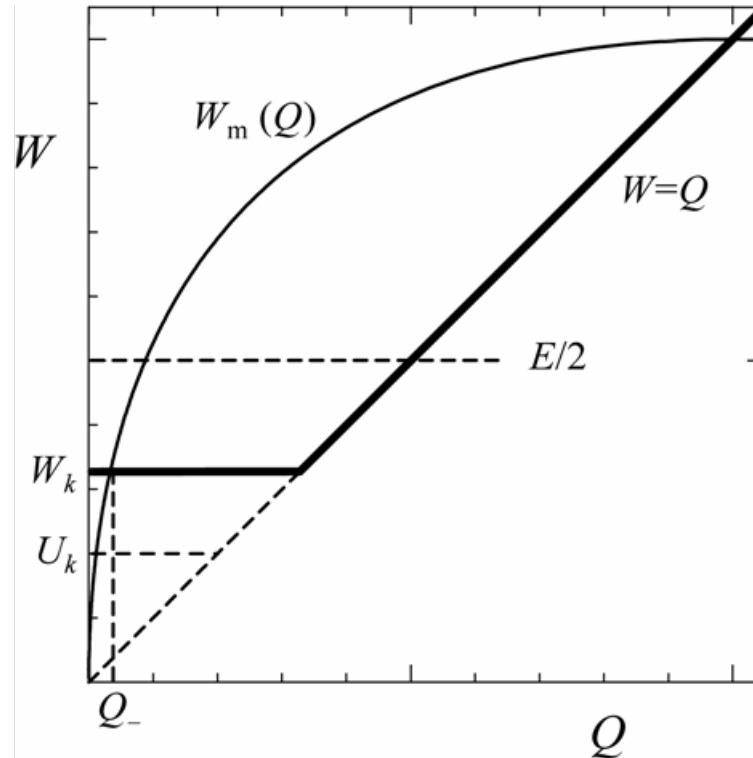
$df(Q,W)/dW$ is known analytically only for H and the free-electron gas

□ Sternheimer-Liljequist GOS model

Sum of “delta” oscillators (one per each electron shell)

$$\frac{df(Q, W)}{dW} = \sum_k f_k \left[\delta(W - W_k) \Theta(W_k - Q) + \delta(W - Q) \Theta(Q - W_k) \right]$$

“delta” oscillator:



Satisfies:

1) Bethe sum rule:

$$\int_0^\infty \frac{df(Q, W)}{dW} dW = \sum_k f_k = Z \quad \forall Q$$

2) Mean-ionization energy

$$\int_0^\infty \ln W \frac{df(Q, W)}{dW} dW = \sum_k f_k \ln W_k = Z \ln I$$

□ Integrated cross sections

□ Energy-loss DCS

$$\frac{d\sigma_{\text{in}}}{dW} = \int_{Q_-}^{Q_+} \frac{d^2\sigma_{\text{in}}}{dQ dW} dQ \quad Q_{\pm} \equiv Q(\cos\theta = \mp 1)$$

□ Total integrated cross sections

$$\sigma_{\text{in}}^{(n)} = \int_0^{W_{\text{max}}} W^n \frac{d\sigma_{\text{in}}}{dW} dW$$

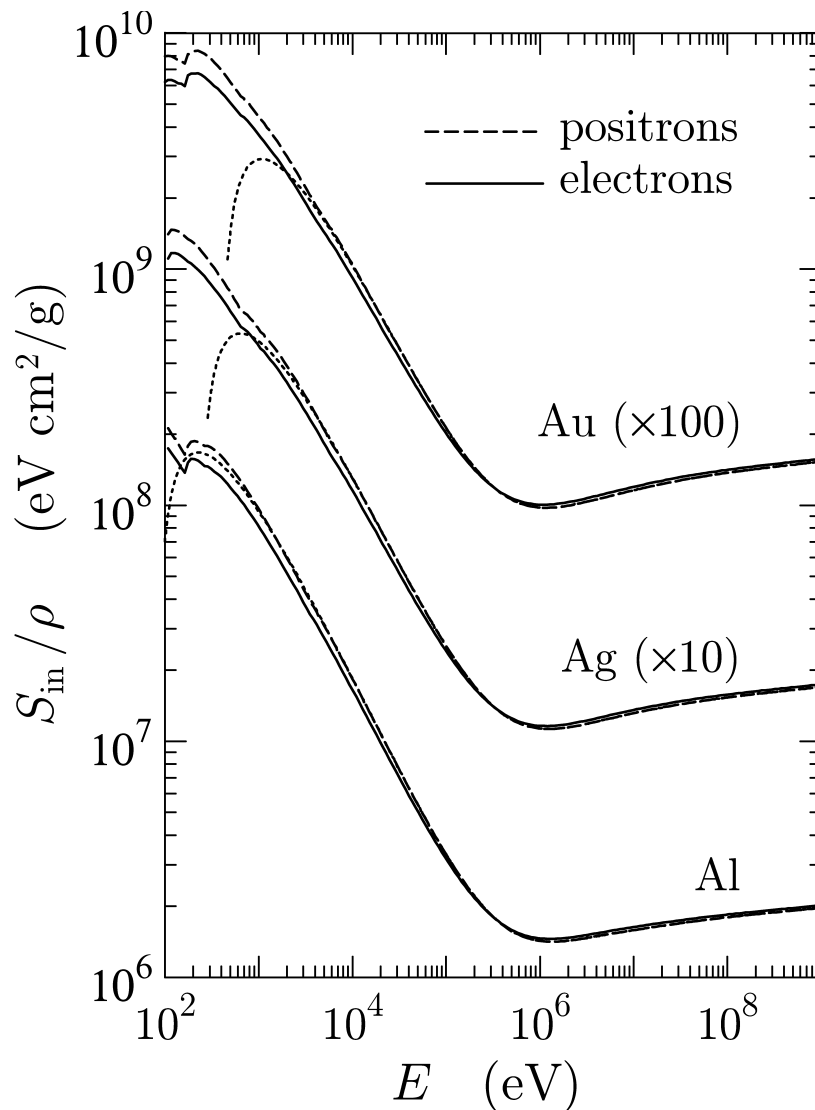
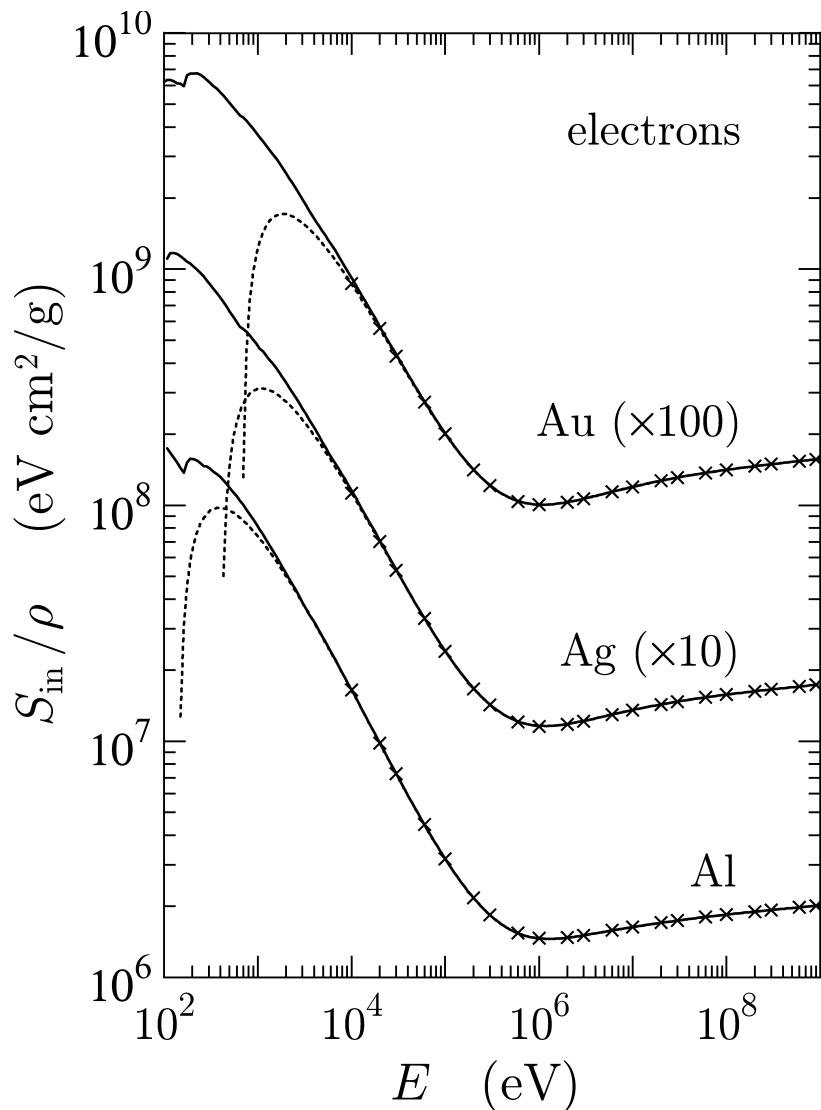
Inelastic mean free path, stopping power and energy straggling parameter

$$\lambda_{\text{in}}^{-1} = \mathcal{N}\sigma_{\text{in}}^{(0)} \quad S_{\text{in}} = \mathcal{N}\sigma_{\text{in}}^{(1)} = \frac{\langle W \rangle}{\lambda_{\text{in}}} \quad \Omega_{\text{in}}^2 = \mathcal{N}\sigma_{\text{in}}^{(2)} = \frac{\langle W^2 \rangle}{\lambda_{\text{in}}}$$

All calculations are performed analytically

In the high-energy limit, the Bethe stopping power formula is obtained, but our model is valid down to lower energies

Collision stopping powers



Continuous and dashed curves: present GOS model.

Crosses: ICRU 37 data.

Dotted curves: Bethe formula

□ Bremsstrahlung emission

Charged projectiles, accelerated by the electrostatic field of the target atom emit electromagnetic radiation

□ **Bethe-Heitler energy-loss DCS** (Plane-wave Born approximation)

$$\frac{d\sigma_{\text{br}}^{(\text{BH})}}{dW} \propto \alpha Z(Z + \eta) \frac{1}{W}$$

DCS for electrons:

$$\frac{d\sigma_{\text{br}}}{dW} = \frac{Z^2}{\beta^2} \frac{1}{W} \chi(Z, E, \kappa)$$

$\chi(Z, E, \kappa) = (\beta^2/Z^2)W d\sigma_{\text{br}}/dW$ "scaled" bremsstrahlung DCS

$\kappa = W/E$ reduced photon energy $\in (0, 1)$

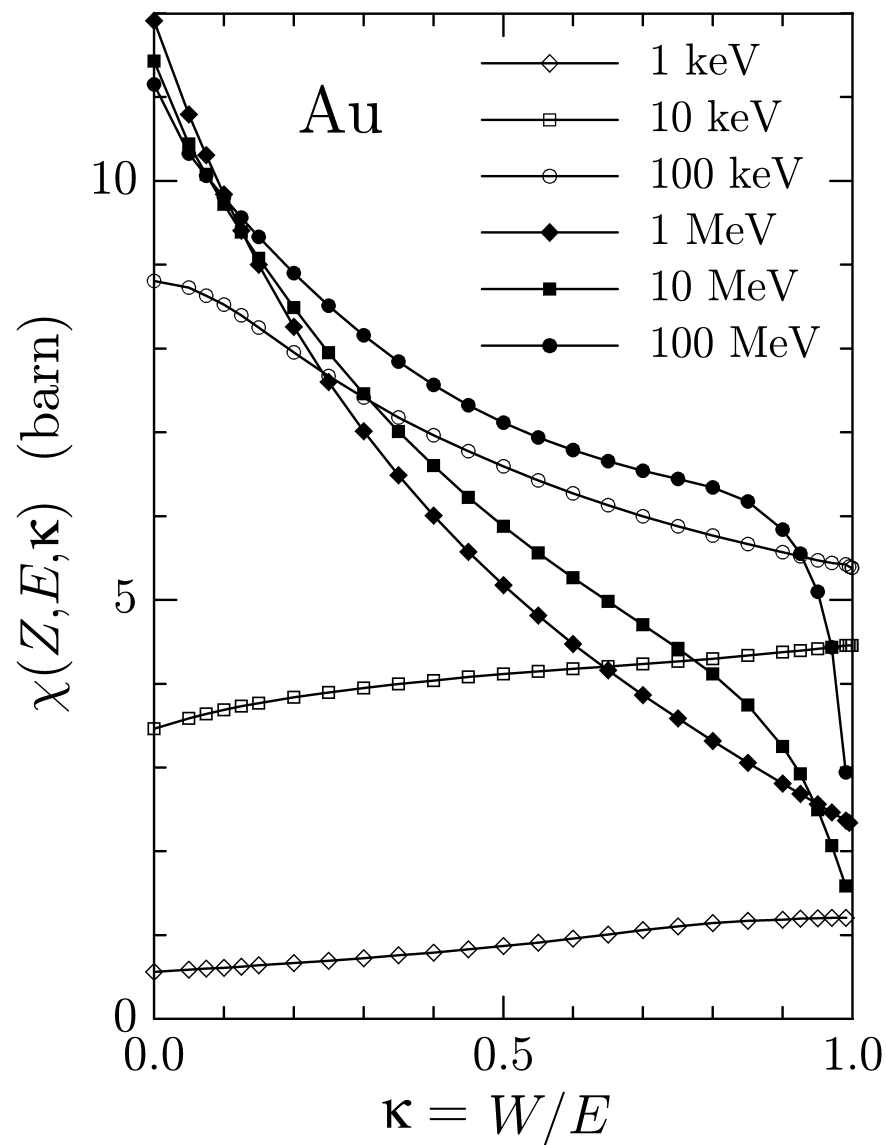
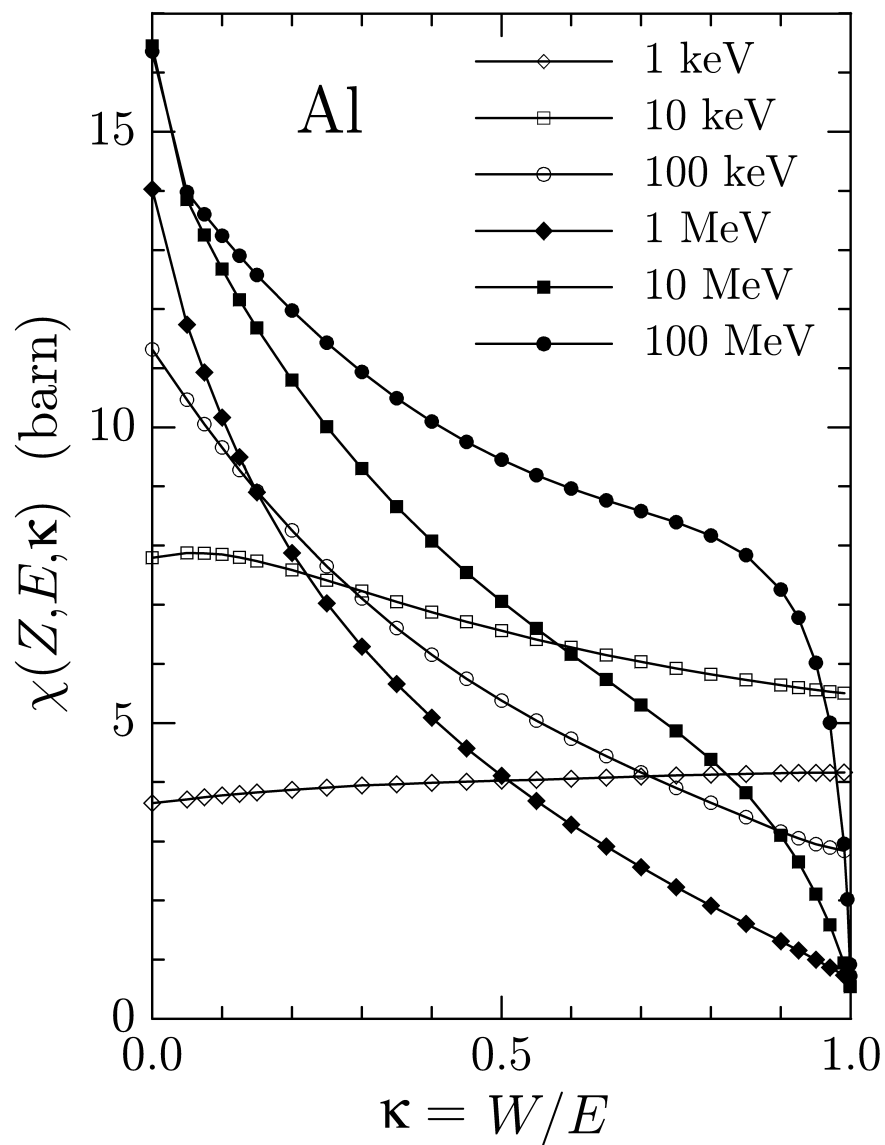
Seltzer and Berger (1986) tables of $\chi(Z, E, \kappa)$

- electron-nucleus: Bethe-Heitler DCS

combined with partial-wave calculations by Pratt et al. (1977)

- electron-electron: Haug (1975) theory

□ Scaled bremsstrahlung DCSs for e^-



Seltzer and Berger (1986)

□ Integrated cross sections

Mean free path (restricted)

$$\kappa_{\text{cr}} \equiv W_{\text{cr}}/E$$

$$\lambda_{\text{br}}^{-1}(E; W_{\text{cr}}) \equiv \mathcal{N} \int_{W_{\text{cr}}}^E \frac{d\sigma_{\text{br}}}{dW} dW = \mathcal{N} \frac{Z^2}{\beta^2} \int_{\kappa_{\text{cr}}}^1 \frac{1}{\kappa} \chi(Z, E, \kappa) d\kappa$$

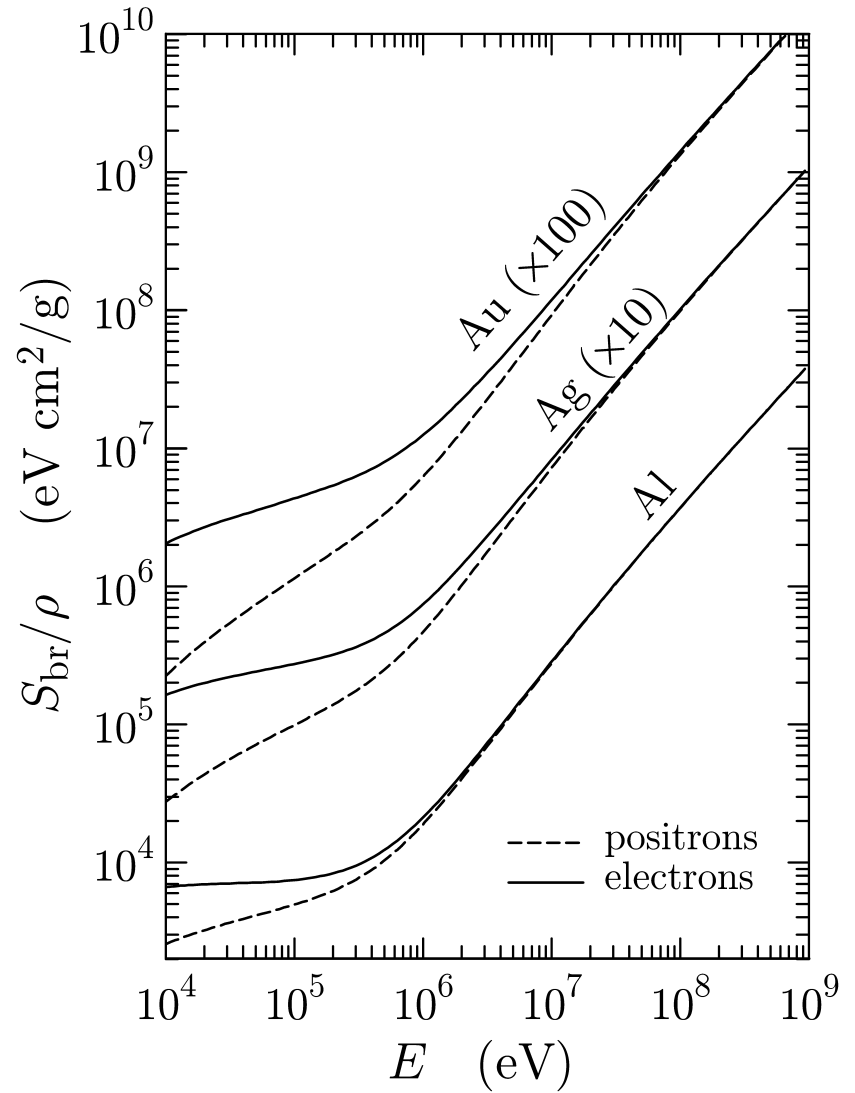
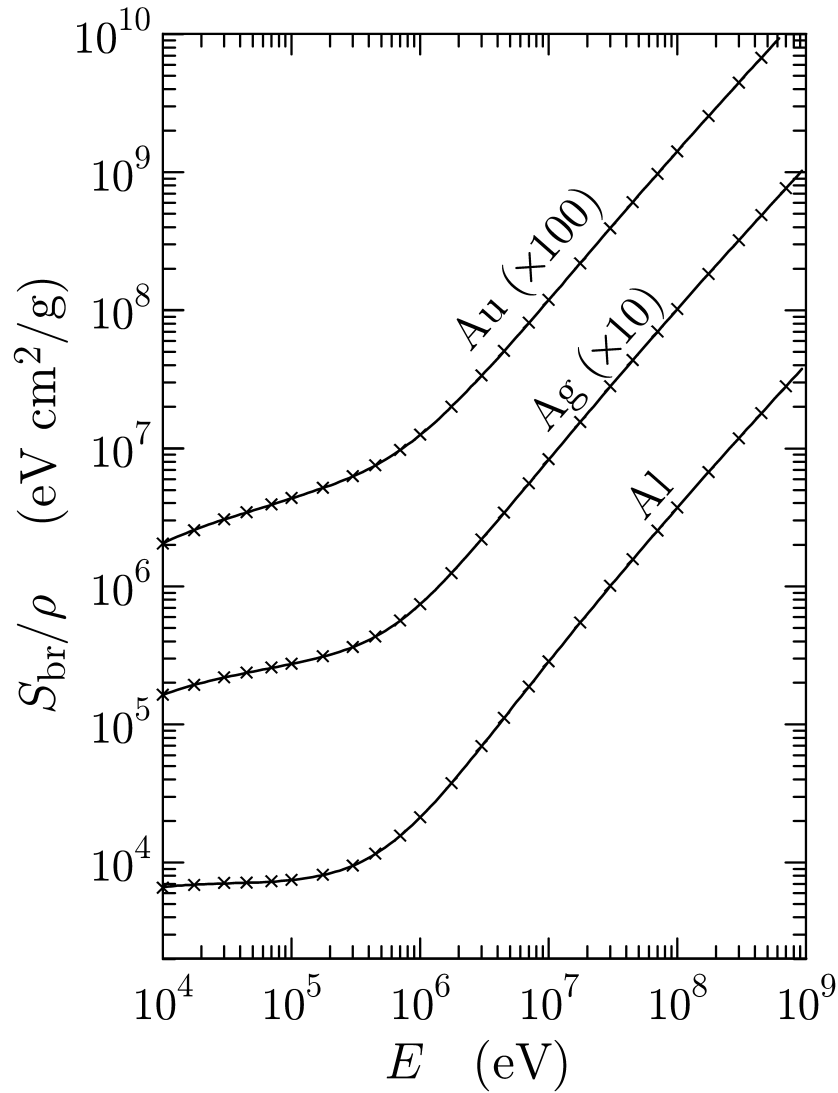
Radiative stopping power

$$S_{\text{br}}(E) \equiv \mathcal{N} \int_0^E W \frac{d\sigma_{\text{br}}}{dW} dW = \mathcal{N} \frac{Z^2}{\beta^2} E \int_0^1 \chi(Z, E, \kappa) d\kappa$$

Bremsstrahlung straggling parameter

$$\Omega_{\text{br}}^2(E) \equiv \mathcal{N} \int_0^E W^2 \frac{d\sigma_{\text{br}}}{dW} dW = \mathcal{N} \frac{Z^2}{\beta^2} E^2 \int_0^1 \kappa \chi(Z, E, \kappa) d\kappa$$

□ Radiative stopping powers



Continuous and dashed curves: present model.

Crosses: ICRU 37 data.

□ Angular distribution of emitted photons

Double DCS

$$\frac{d^2\sigma_{\text{br}}}{dW d(\cos\theta)} = \frac{d\sigma_{\text{br}}}{dW} p(Z, E, \kappa; \cos\theta)$$

$p(Z, E, \kappa; \cos\theta)$ = shape function (pdf, normalized to unity)

Partial-wave calculations of shape functions (Kissel et al., 1983):

$$Z = 2, 8, 13, 47, 79, 92$$

$$E = 1, 5, 10, 50, 100, 500 \text{ keV}$$

$$\kappa = 0, 0.6, 0.8, 0.95$$

+ parameterization in terms of Legendre polynomials (not useful)

Kirkpatrick-Wiedmann-Statham formula

$$p^{(\text{KWS})}(Z, E, \kappa; \cos\theta) = \frac{\sigma_x(1 - \cos^2\theta) + \sigma_y(1 + \cos^2\theta)}{(1 - \beta \cos\theta)^2}$$

Ansatz for the shape function in K' = reference frame moving with the e^\pm

$$p_d(\cos \theta') = A \frac{3}{8} (1 + \cos^2 \theta') + (1 - A) \frac{3}{4} (1 - \cos^2 \theta') \quad 0 \leq A \leq 1$$

Lorentz transformation to K = laboratory reference frame

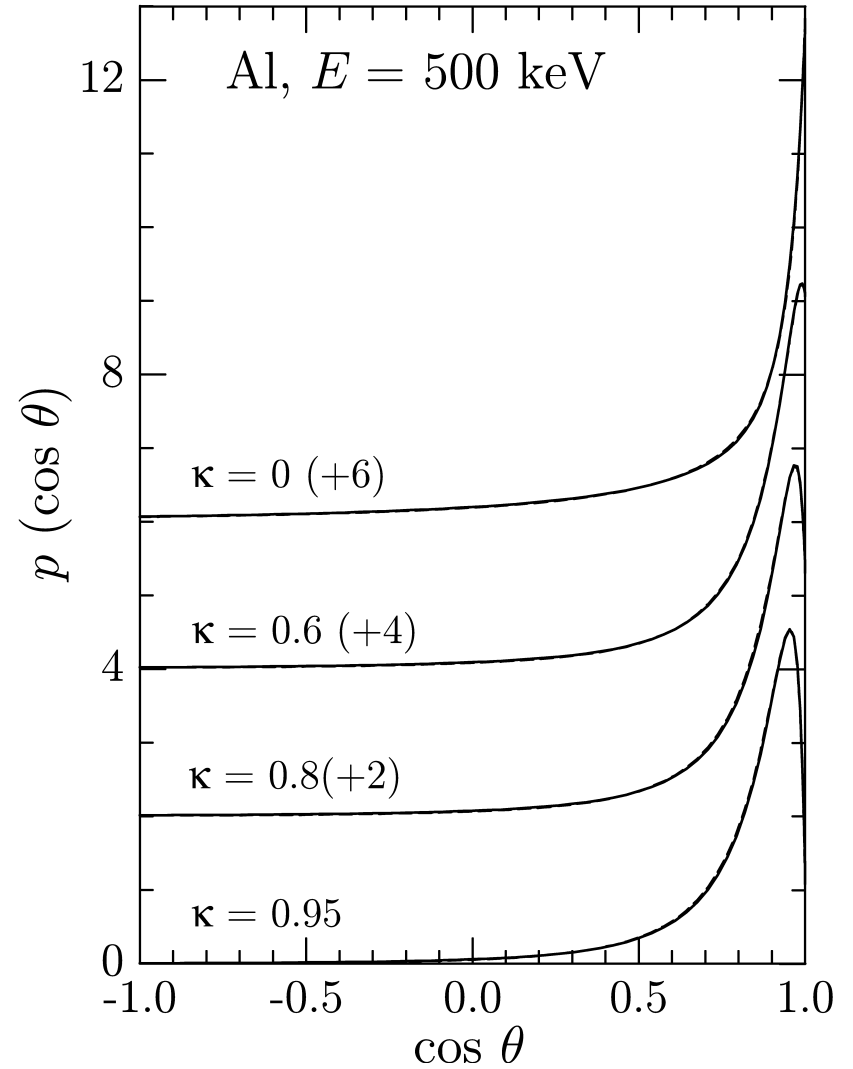
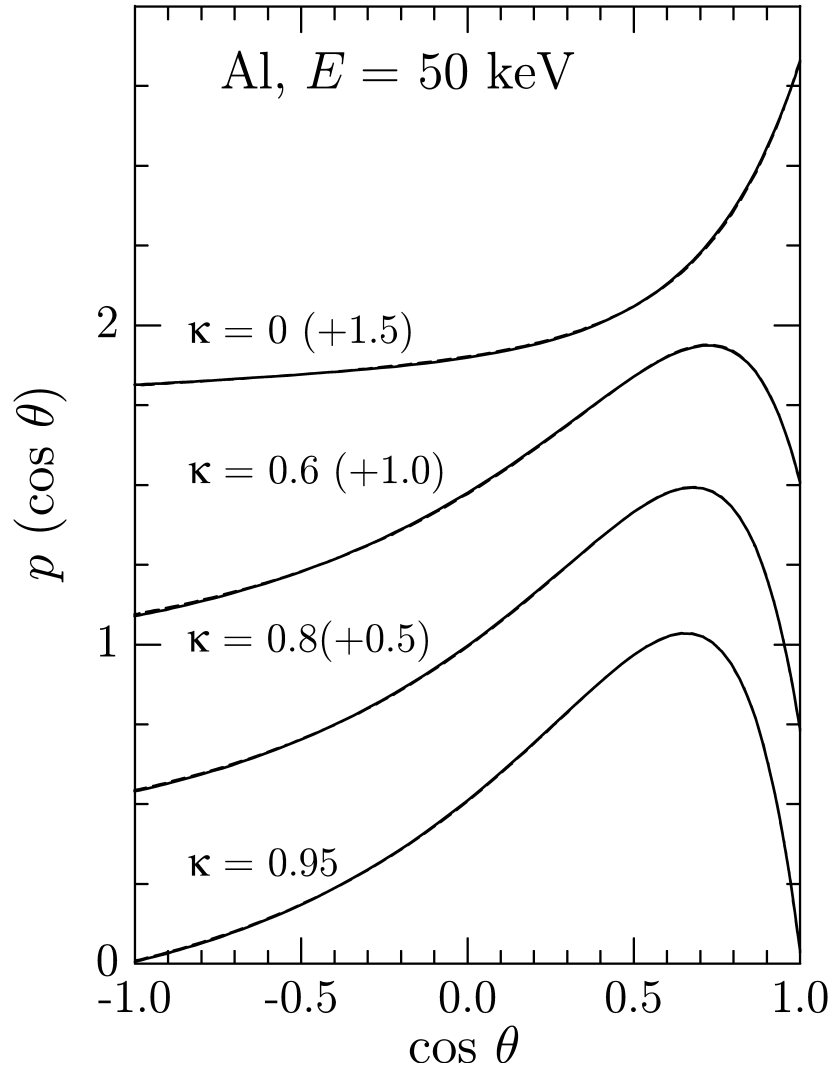
$$\cos \theta = \frac{\cos \theta' + \beta}{1 + \beta \cos \theta'} \quad \phi = \phi'$$

the angular distribution in K reads

$$\begin{aligned} p(\cos \theta) &= p_d(\cos \theta') \frac{d(\cos \theta')}{d(\cos \theta)} \\ &= A \frac{3}{8} \left[1 + \left(\frac{\cos \theta - \beta}{1 - \beta \cos \theta} \right)^2 \right] \frac{1 - \beta^2}{(1 - \beta \cos \theta)^2} \\ &\quad + (1 - A) \frac{3}{4} \left[1 - \left(\frac{\cos \theta - \beta}{1 - \beta \cos \theta} \right)^2 \right] \frac{1 - \beta^2}{(1 - \beta \cos \theta)^2} \end{aligned}$$

A and β are adjustable parameters

Shape functions for bremsstrahlung emission in Al



Dashed curves: partial-wave calculations by Kissel et al. (1983)

Continuous curves: analytical fit

□ Secondary electron (delta ray) emission

□ Initial energy

For ionization of inner shells ($i = K, L1-L3, M1-M5$) $E_s = W - U_i$

outer shells ($i = N, O, \dots, cb$) $E_s = W$

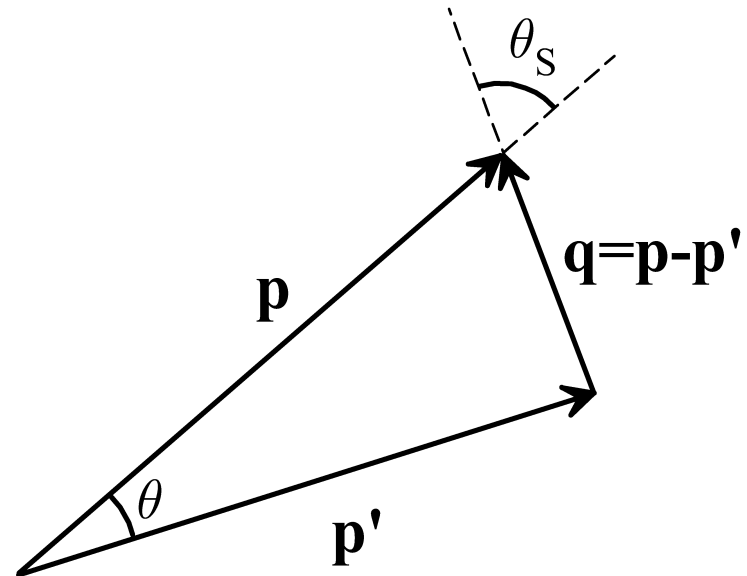
□ Initial direction

The secondary electron is emitted in the direction of the momentum transfer (Doppler broadening is ignored)

$$\theta_s = \theta_r, \quad \phi_s = \phi + \pi$$

In the case of close collisions

$$\cos \theta_s (Q = W) = \left(\frac{W}{E} \frac{E + 2m_e c^2}{W + 2m_e c^2} \right)^{1/2}$$



The projectile changes direction and energy and the delta ray is emitted ... but the de-excitation of the ionized target is not followed (see below)

□ Ionization of inner shells by e^\pm impact

The single delta-oscillator model is not accurate enough to describe inner-shell ionization (production of x-rays and Auger electrons)

Inner-shell ionization is simulated as an **independent process**, which does not affect the state of the projectile; to follow the relaxation of the target ion (x-rays and Auger electrons). Only the total cross section is needed.

□ Weizsäcker-Williams method of virtual quanta

Continuous superposition of oscillators

$$\frac{df_i(Q, W)}{dW} \equiv \int_{U_i}^{\infty} \frac{df_i(W')}{dW'} F_\delta(W'; Q, W) dW' + Z_r \delta(W - Q) \Theta(W - U_i)$$

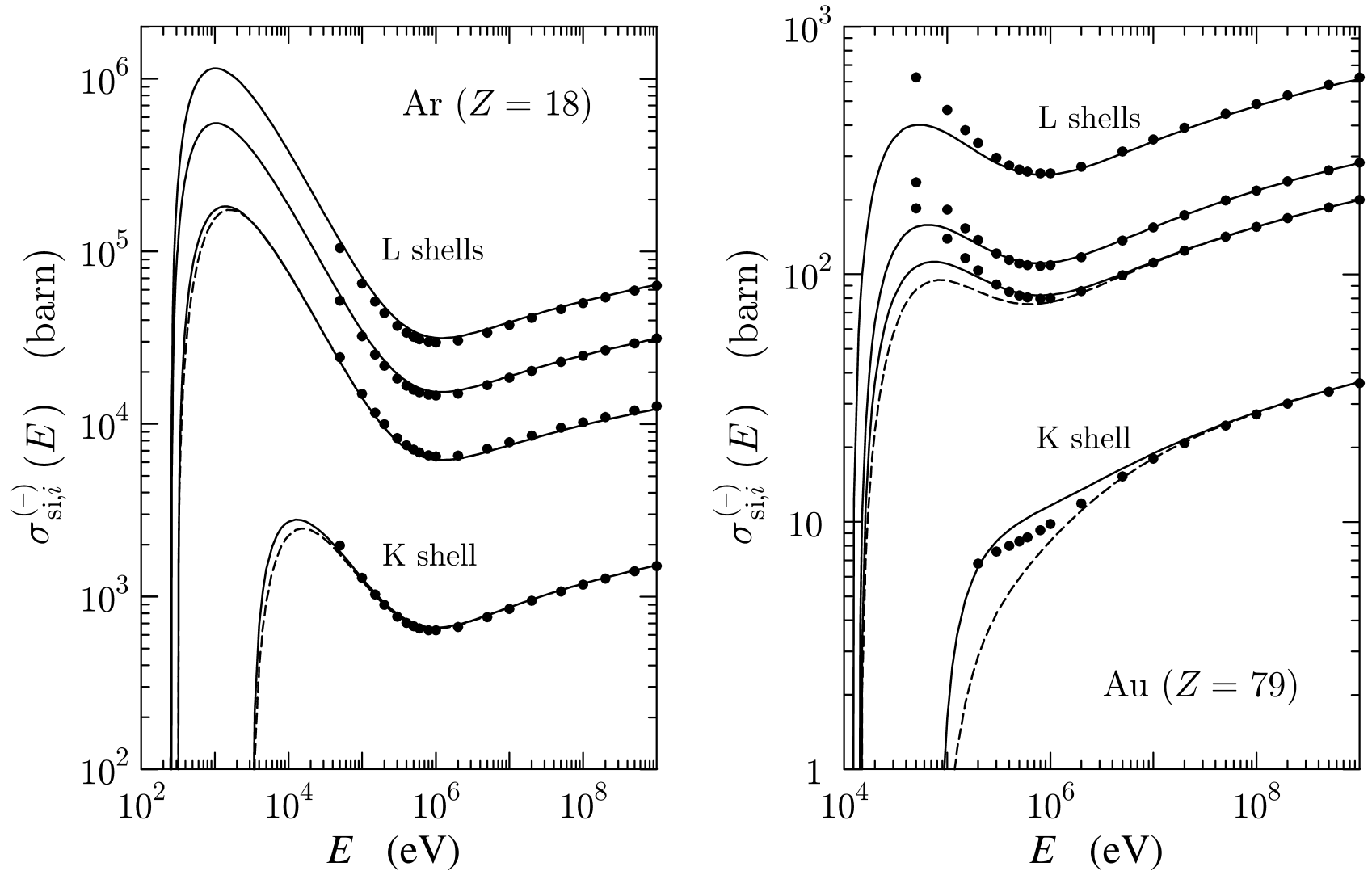
$$\frac{df_i(W)}{dW} = \frac{m_e c}{2\pi^2 e^2 \hbar} \sigma_{\text{ph},i}(Z, W) \quad Z_r = Z_i - \int_{U_i}^{\infty} \frac{df_i(W')}{dW'} dW'$$

Low-energy exchange and distortion corrections are applied

The results for K, L and M shells are equivalent to those from the Born approximation with independent-electron models. Reliable for $E \gg U_i$

For lower energies: distorted-wave Born approximation (version 2008)

Ionization cross sections by electron impact



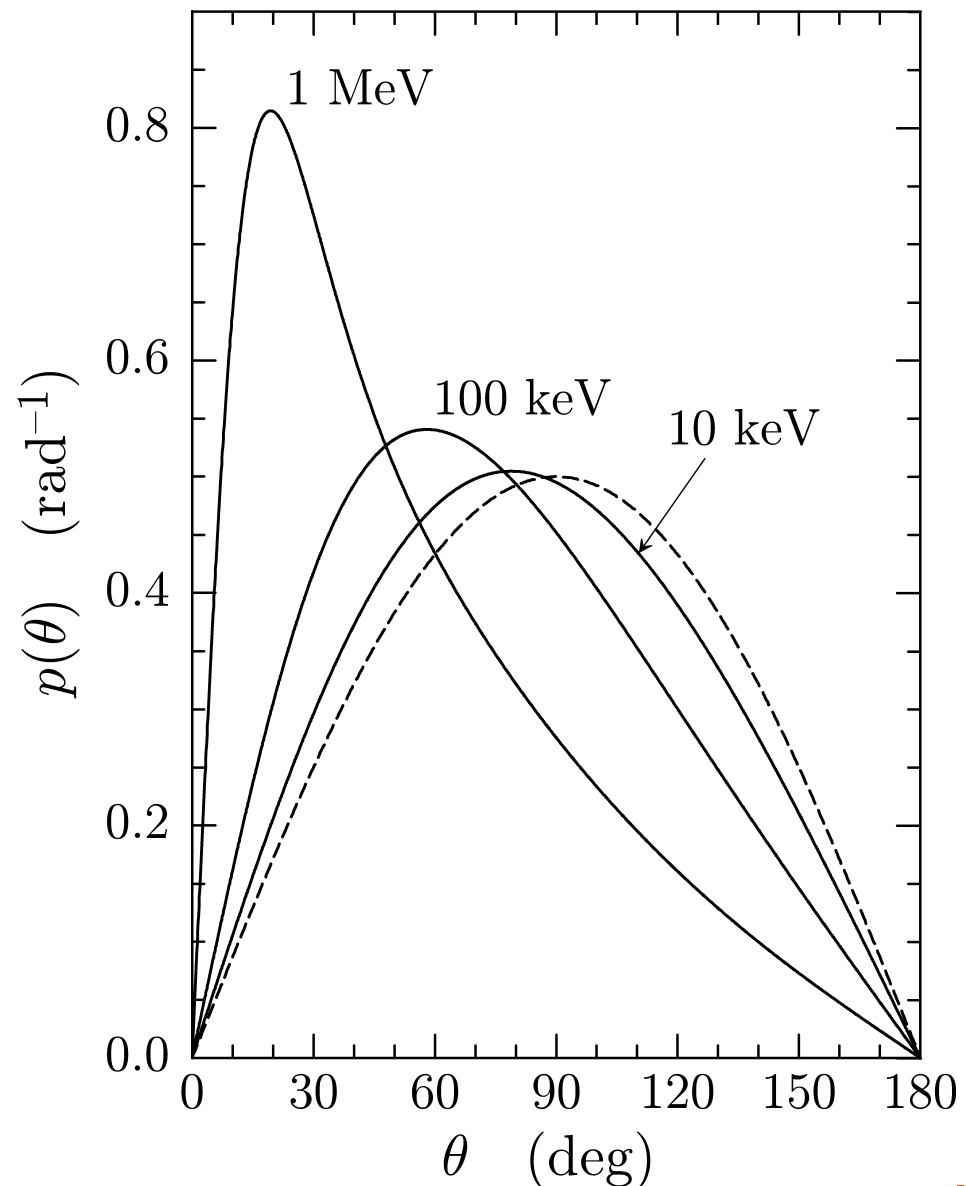
Continuous and dashed curves: WW method for electrons and positrons
Dots: First-principles Born approximation results of Scofield

□ Positron annihilation

□ Heitler (two-photon) DCS

The positron may annihilate either in flight or at rest

Continuous curves: in flight
Dashed curve: isotropic distribution



❑ Mixed (class II) simulation algorithms

We define (small) angle and energy-loss cutoffs (θ_c, W_c) and consider:

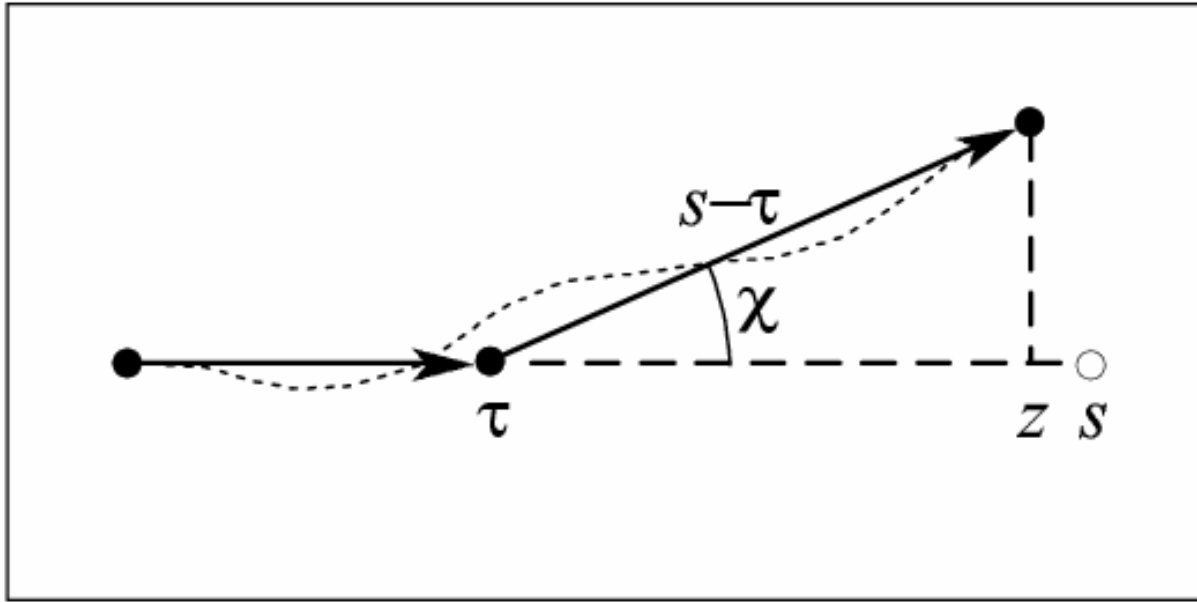
- ❑ Hard collisions: with $\theta > \theta_c$ or $W > W_c$, only a few in each electron history
Detailed simulation is inexpensive
- ❑ Soft collisions: with $\theta < \theta_c$ and $W < W_c$, a large number (on average) between each pair of hard interactions

❑ Advantages of mixed algorithms

- ❑ Hard interactions are simulated “exactly”
- ❑ Condensed simulation of soft events is reliable:
 - Small-angle approximation
 - Gaussian E straggling
 - The random-hinge method is well suited to describe spatial displ.
- ❑ Easy, and fairly accurate, description of interface crossings
- ❑ Very stable with respect to the cutoffs

□ Random-hinge method

Correlation between angular deflection and space displacements



$$\langle z \rangle_{\text{sim}}^{(s)} = \frac{s}{2} + \frac{s}{2} \langle \cos \chi \rangle^{(s)} = s \left[1 - \frac{1}{2} \left(\frac{s}{\lambda_{\text{el},1}^{(s)}} \right) + \frac{1}{4} \left(\frac{s}{\lambda_{\text{el},1}^{(s)}} \right)^2 - \dots \right]$$

$$s \ll \lambda_{\text{el},1}^{(s)}$$

$$\langle x^2 + y^2 \rangle_{\text{sim}}^{(s)} = \langle (s - \tau)^2 \sin^2 \chi \rangle_{\text{sim}}^{(s)} = \frac{2}{9} \frac{s^3}{\lambda_{\text{el},2}^{(s)}} \left[1 - \frac{1}{2} \frac{\lambda_{\text{el},1}^{(s)}}{\lambda_{\text{el},2}^{(s)}} \left(\frac{s}{\lambda_{\text{el},1}^{(s)}} \right) + \dots \right]$$

□ Soft energy-loss events

□ Central-limit theorem

$$G(s; w) \simeq \frac{1}{\sqrt{2\pi\Omega_s^2 s}} \exp \left[-\frac{(w - S_s s)^2}{2\Omega_s^2 s} \right]$$

... but we must have $\sqrt{\Omega_s^2 s} \ll S_s s \ll E \Rightarrow$

$$s > s_{\text{crit}} = \Omega_s^2 / S_s^2$$

When this condition is not satisfied, we use “artificial” distributions with the correct first and second moments

NOTES: 1) Consistent only when there are multiple soft events
2) w is bound; $w \leq \langle w \rangle + 3\sigma$

... accurate only when $w \ll E$!

□ Simulation parameters

$$C_1, C_2, W_{cc}, W_{cr}, s_{max}$$

- $0 \leq C_1 \leq 0.2$
- $0 \leq C_2 \leq 0.2$ (effective only at very high energies)
- W_{cc} and W_{cr} (“estimated” from experiment/scoring details)
- s_{max} (to ensure multiple soft interactions, to allow energy-loss corrections, transport in EM fields)

When the input W_{cr} is negative, PENELOPE sets $W_{cr} = 10$ eV and soft bremsstrahlung is switched off

$$C_1 = C_2 = W_{cc} = s_{max} = 0, W_{cr} = -10 \text{ eV} \Rightarrow \text{detailed simulation}$$

□ Stability

Example: 500 keV electrons in Al. $s = 200 \mu\text{m}$.

• Detailed simulation

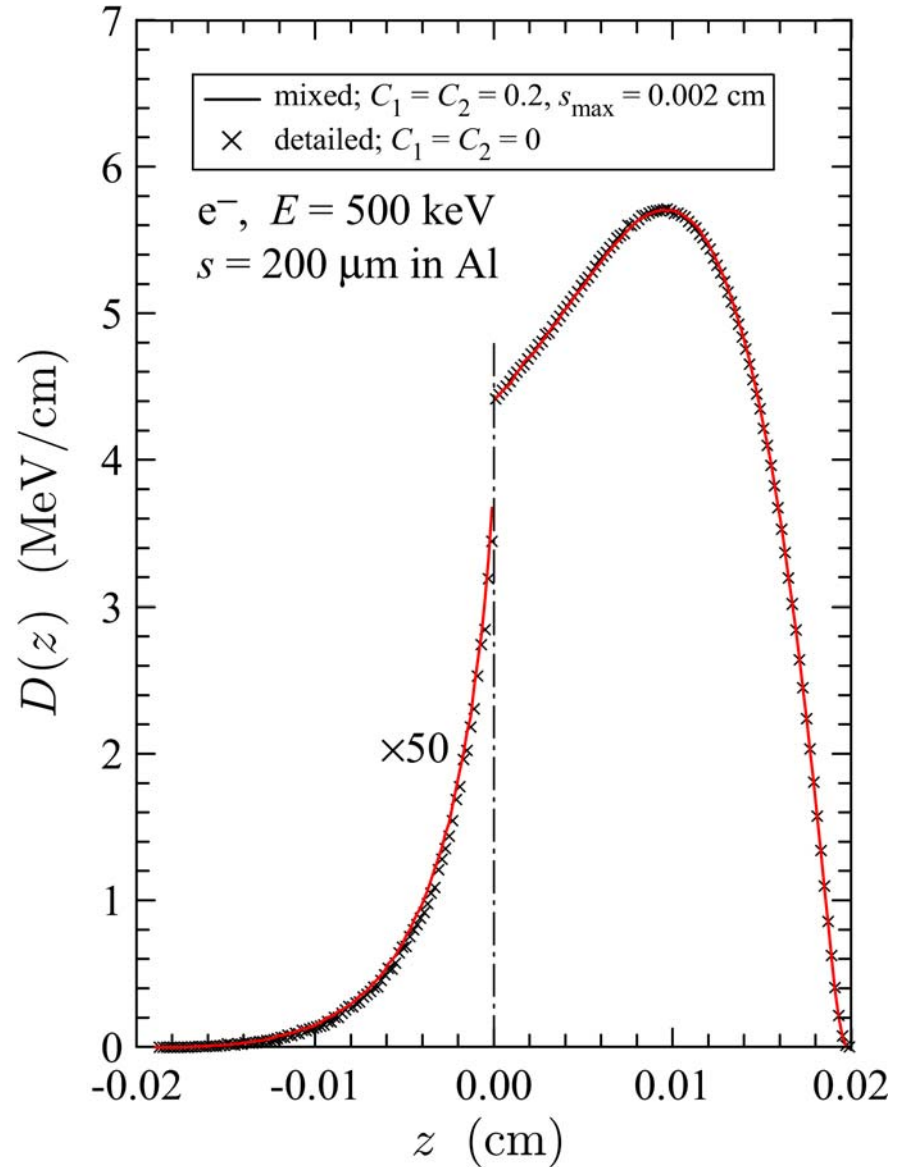
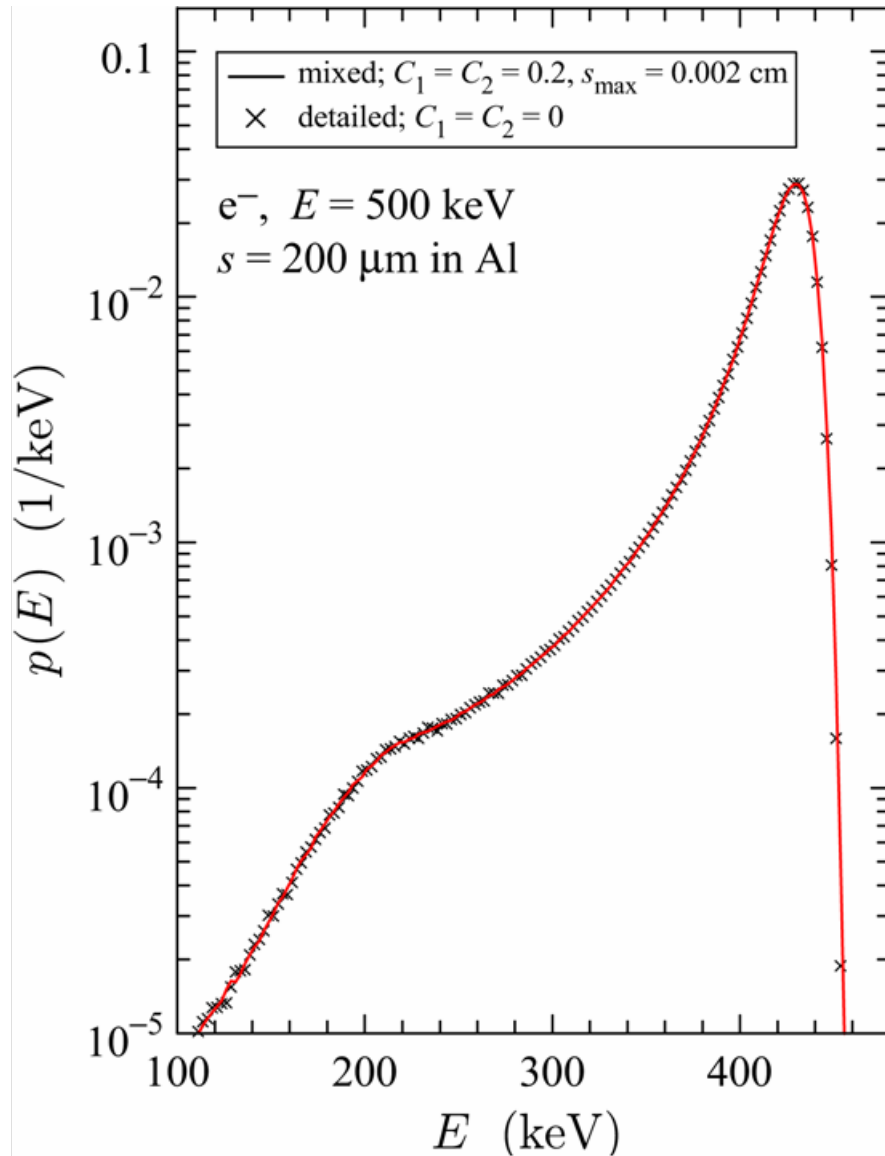
$$\begin{aligned} C_1 = C_2 = 0; & \quad W_{\text{cc}} = 0 \text{ eV} \\ W_{\text{cr}} = -100 \text{ eV} & \quad (\text{soft bremsstrahlung disregarded}) \end{aligned}$$

• Mixed simulation

$$\begin{aligned} C_1 = C_2 = 0.2 & \quad (\text{extreme case!}) \\ W_{\text{cc}} = 1 \text{ keV}; & \quad W_{\text{cr}} = -100 \text{ eV} \quad (\text{soft bremsstrahlung disregarded}) \\ s_{\text{max}} = 20 \mu\text{m} & \end{aligned}$$

about 75 times faster

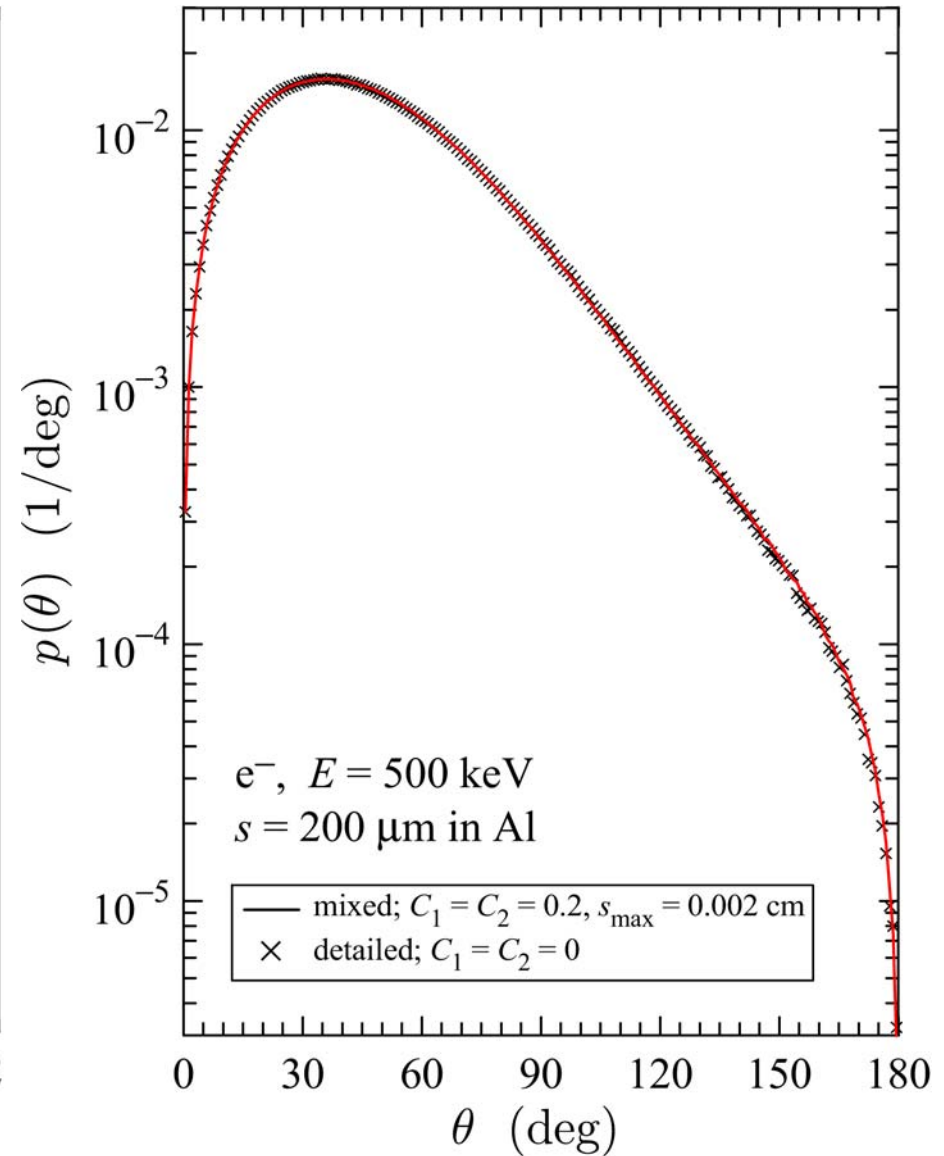
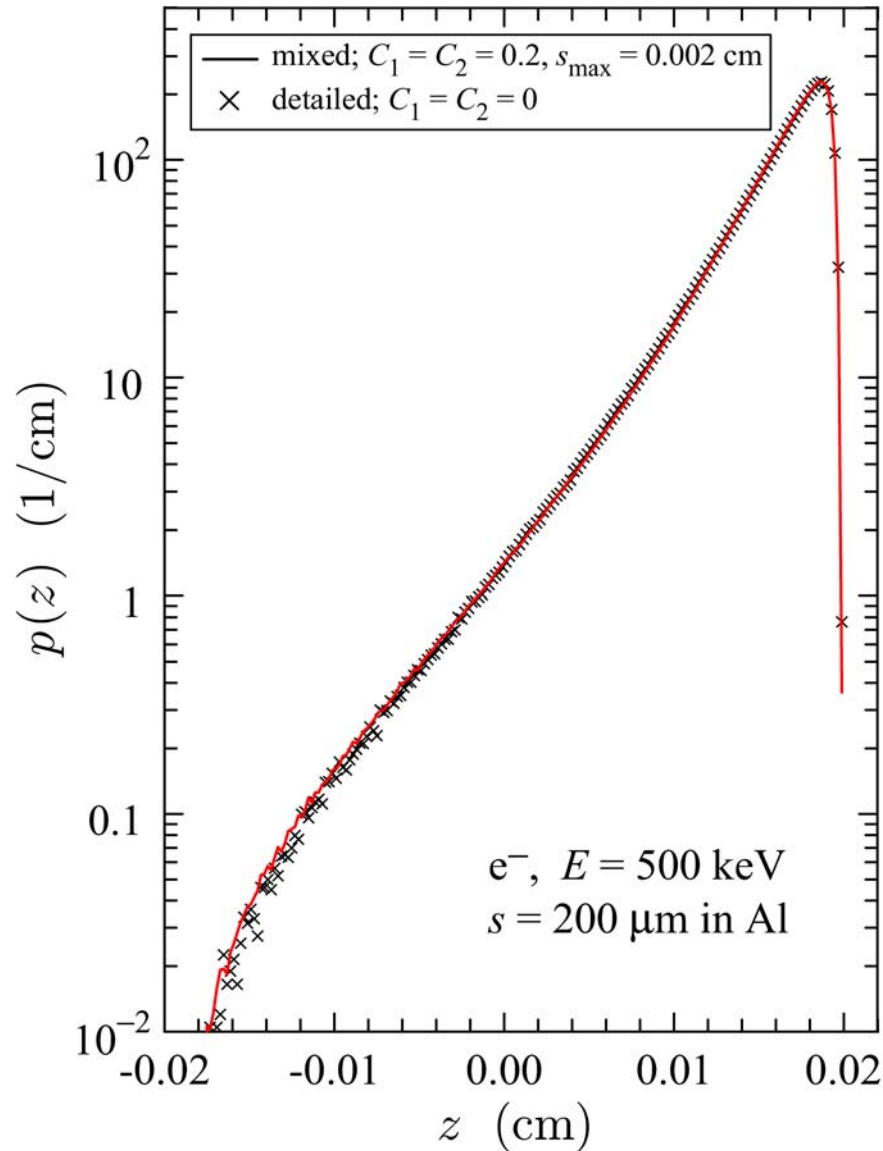
□ Detailed vs. mixed simulation



crosses: detailed simulation

solid lines: mixed simulation

□ Detailed vs. mixed simulation



crosses: detailed simulation

solid lines: mixed simulation

❑ Constructive quadric geometry

❑ PENGEOM

Arbitrary systems consisting of homogeneous bodies limited by quadric surfaces

$$\begin{aligned}\Phi(\mathbf{r}) = & A_{xx}x^2 + A_{yy}y^2 + A_{zz}z^2 + A_{xy}xy + A_{xz}xz + A_{yz}yz \\ & + A_x x + A_y y + A_z z + A_0 = 0\end{aligned}$$

❑ Definition of surfaces

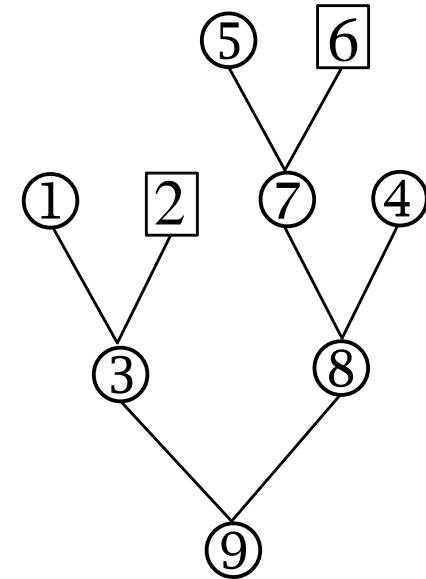
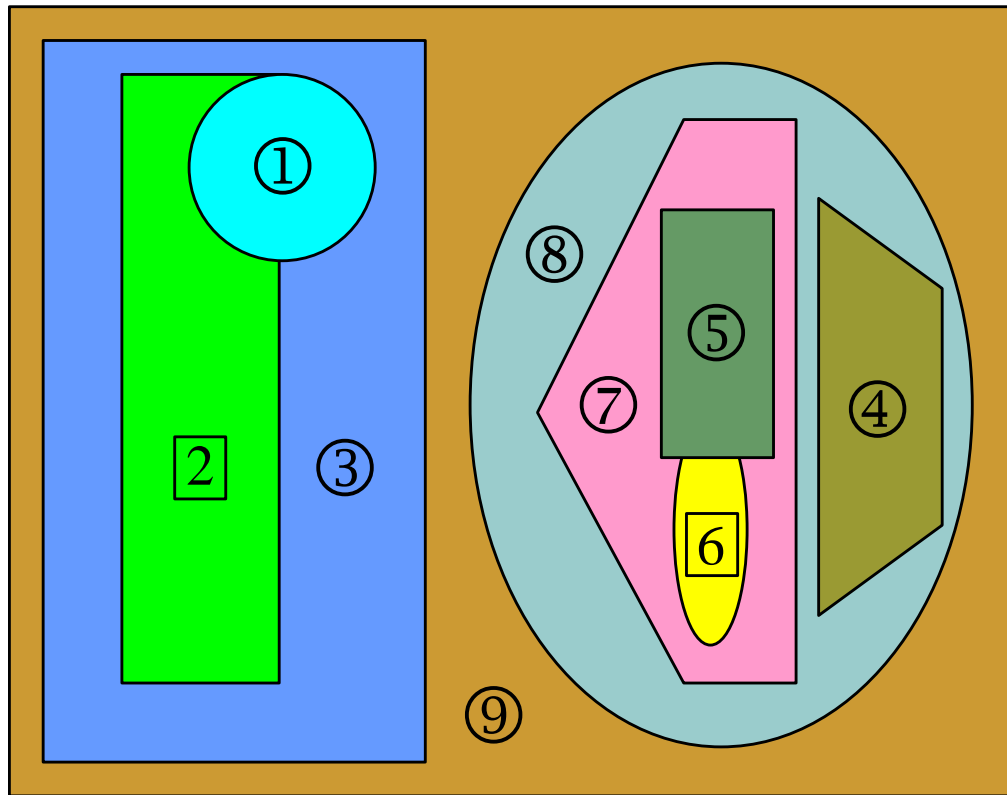
- ❑ Implicit or reduced form
- ❑ Transformations: scaling, rotation, translation

❑ Modular structure

- ❑ Bodies
- ❑ Modules (can be cloned and transformed)

Up to 10,000 surfaces and 5,000 bodies and modules

□ Genealogical tree



○ → modules (may have descendants, or not)

□ → bodies

To speed up the simulation, each module should have a small number of daughters (small number of branches in each node).
Simulation speed is almost independent of the complexity of the geometry.

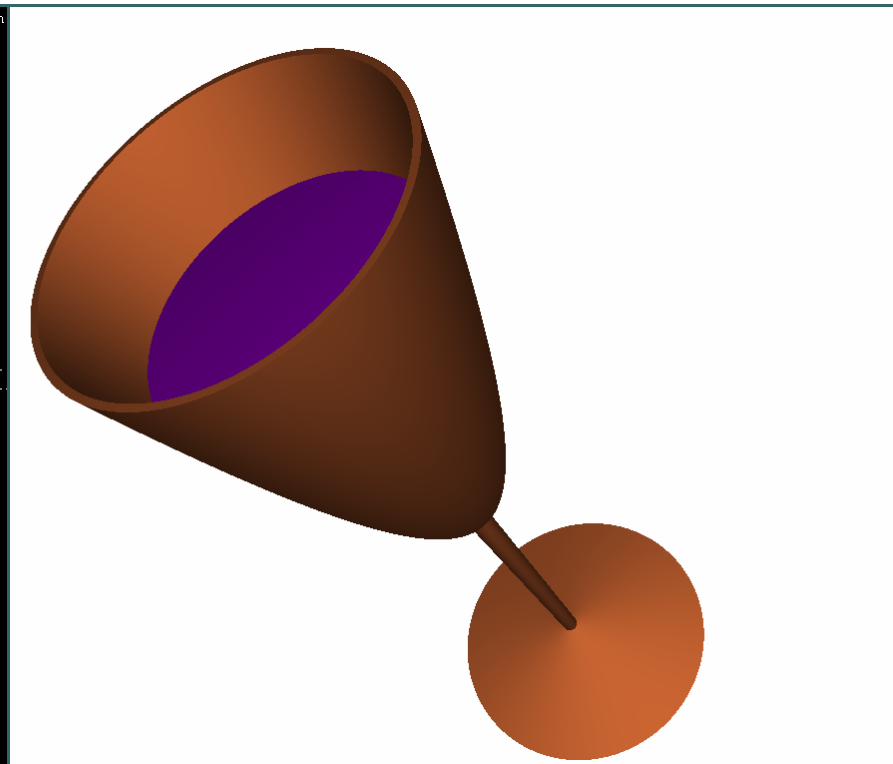
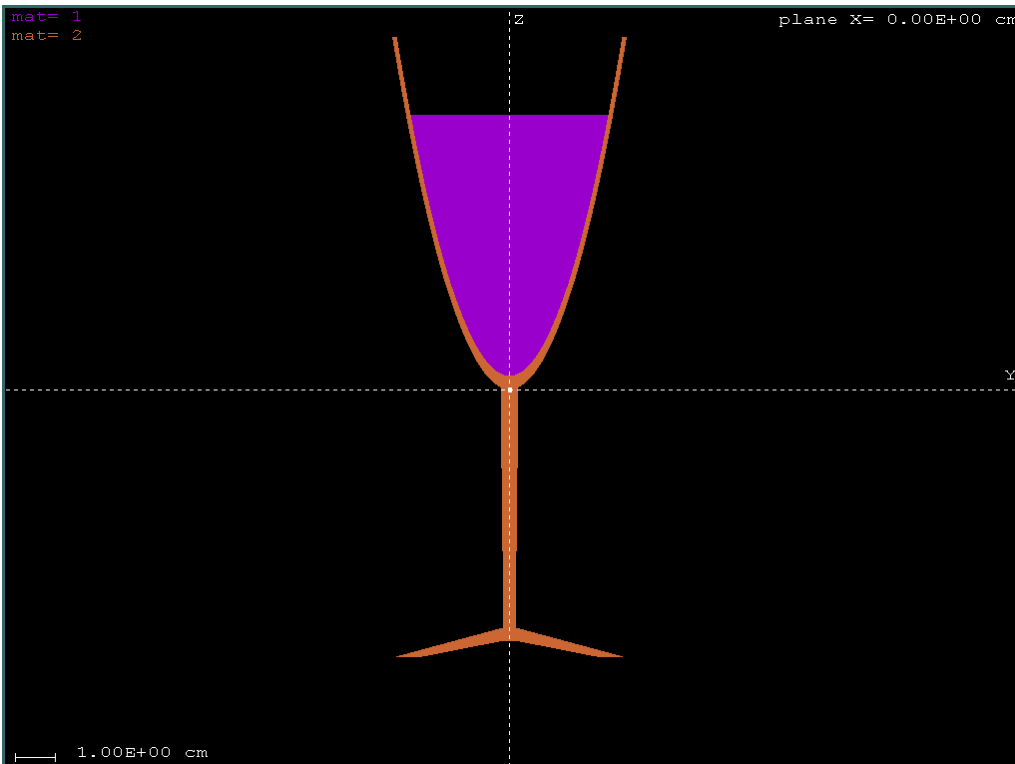
□ Geometry viewers

GVIEW2D two-dimensional (material and body maps)

GVIEW3D three-dimensional images (quite realistic)

They run only under MS Windows.

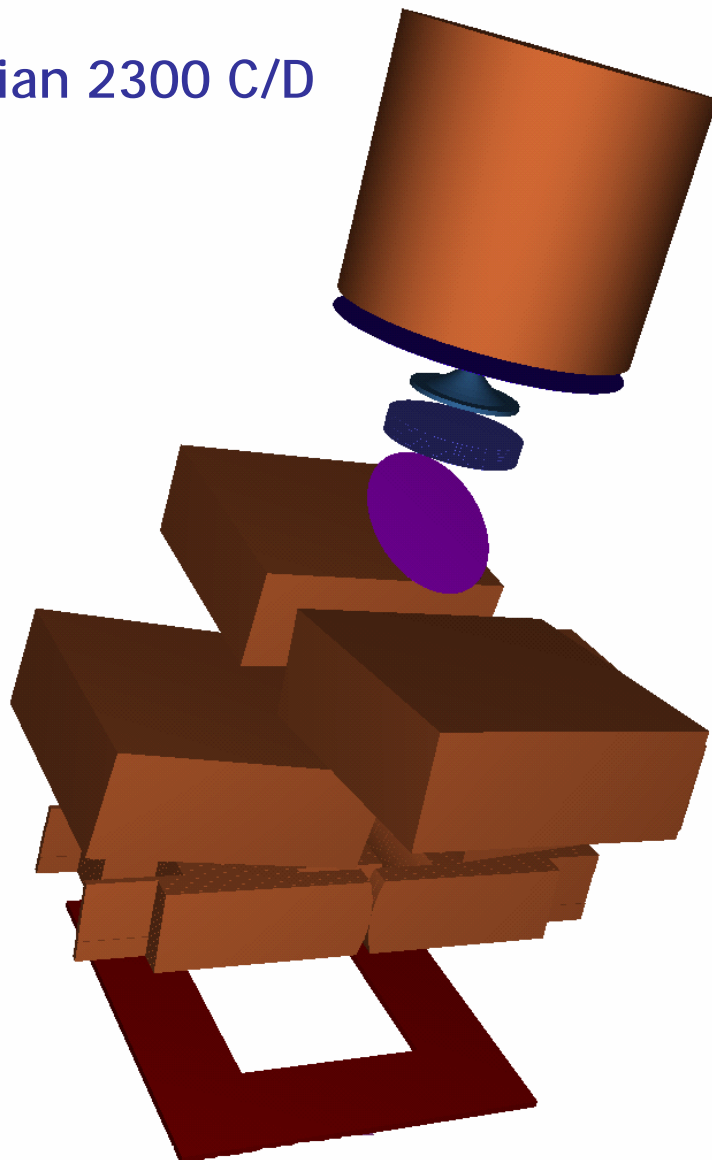
Images generated using the same tracking routines as in the simulation



□ Example: clinical electron accelerators



Varian 2300 C/D



❑ The subroutine package PENGGEOM

User-callable routines

```
SUBROUTINE GEOMIN(PARINP, NPINP, NMAT, NBOD, IRD, IWR)
```

Reads geometry data from the input file, initializes the geometry package and prints the files **geometry.rep** and **pengeom_tree.rep**

```
SUBROUTINE LOCATE
```

Determines the body that contains a point of given coordinates and its material

```
SUBROUTINE STEP(DS, DSEF, NCROSS)
```

Performs the geometrical part of the track simulation. Moves the particle and changes body and material numbers as necessary

□ Impact detectors

SUBROUTINE STEP does not stop particles when they cross an interface between adjacent bodies of the same composition. That is, **these interfaces are not visible from the main program**

```
COMMON /QKDET /KDET (NB)
```

KDET(KB) is initialised to zero. Body **KB** is made part of impact detector **IDET** by setting **KDET(KB)=IDET** (in main program). When particles enter body **KB** coming from a body that is not part of detector **IDET**, they are halted at the surface of the active body and control is returned to the main program.

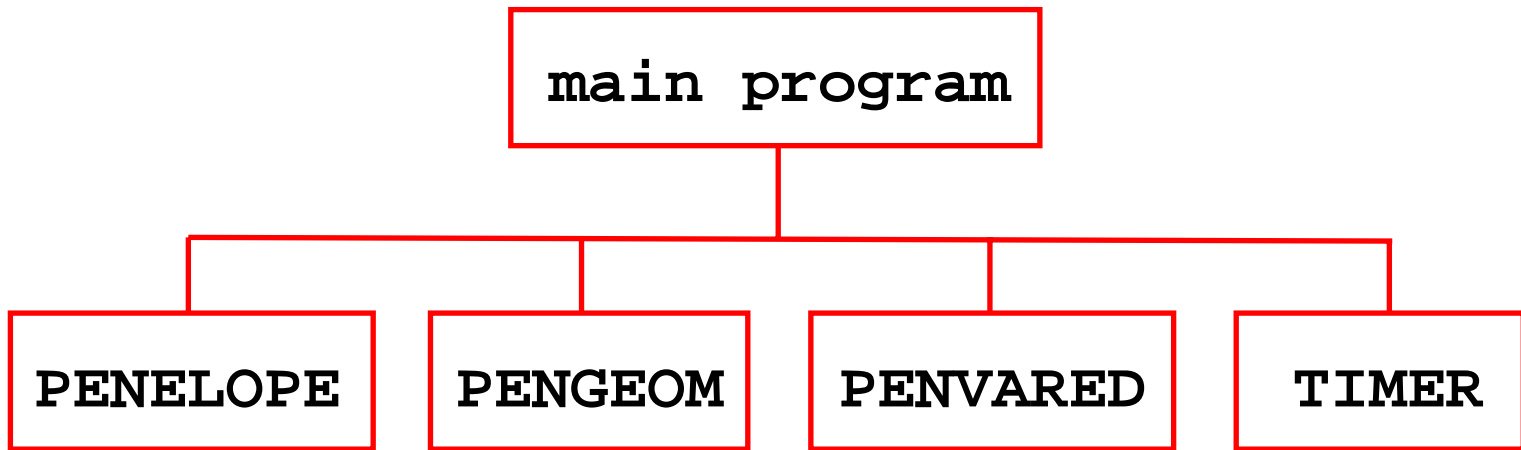
Thus, detector surfaces are made visible from the main program.

Impact detectors are useful for visualising bodies (**GVIEW2D**), for simulating real detectors and for generating phase-space files (**PENMAIN**).

□ Structure of the main program

PENELOPE is a set of Fortran subroutine packages. The user must provide a **steering main program** that generates the initial states of primary particles, controls the evolution of the simulated tracks and keeps score of relevant quantities.

NOTE: the generic main program **penmain** can handle a wide variety of problems, but yours may require some special treatment ...



The communication between the main program and the simulation routines is through a few **common blocks**

Most of the information flux between the main program and the simulation and geometry subroutines is through the common block

```
COMMON/ TRACK/ E, X, Y, Z, U, V, W, WGHT, KPAR, IBODY, MAT, ILB( 5 )
```

which contains the following quantities:

KPAR ... kind of particle (1=electron, 2=photon, 3=positron)
E ... current particle's energy (eV)
X, Y, Z ... position coordinates (cm)
U, V, W ... direction cosines
WGHT ... particle's weight (used only with variance reduction)
IBODY ... index of body where the particle is moving
MAT ... corresponding material
ILB(5) ... describes origin of secondary particles (pp. 215-216)

In the I/O of the PENELOPE and PENGEOM routines, all energies are in **eV** and all lengths are in **cm**

To start the simulation of a particle, its initial state variables must be set by the main program. PENELOPE modifies the energy and direction cosines only when the particle undergoes an interaction. The position coordinates are updated by PENGEOM.

□ The PENELOPE subroutines

SUBROUTINE PEINIT (EPMAX , NMAT , IRD , IWR , INFO)

SUBROUTINE CLEANS

Initializes the secondary stack

SUBROUTINE START

Starts a new shower

SUBROUTINE JUMP (DSMAX , DS)

generate particle histories

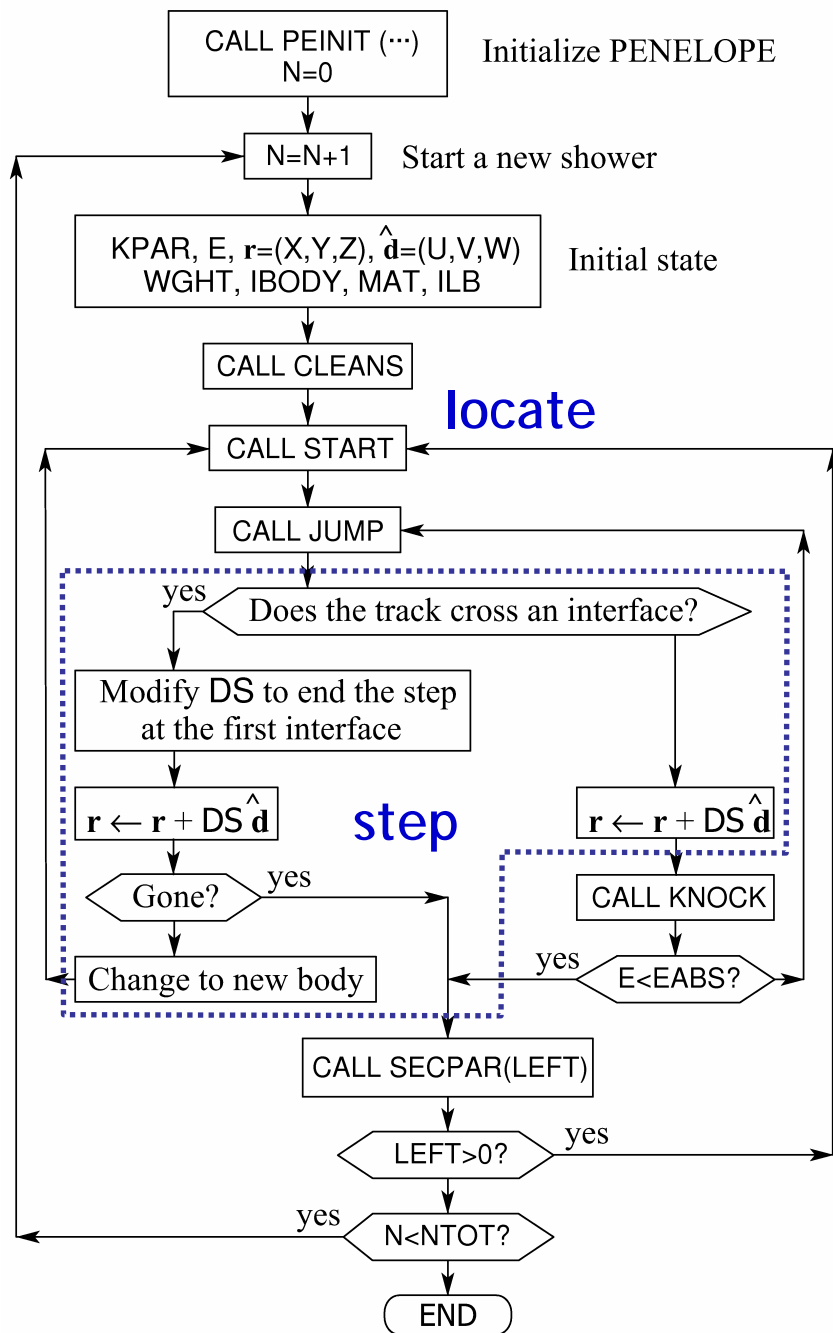
SUBROUTINE KNOCK (DE , ICOL)

SUBROUTINE SECPAR (LEFT)

gets secondary particles from the stack

SUBROUTINE STORES (E , X , Y , Z , U , V , W , WGHT , KPAR , ILB)

stores particles in the stack (splitting)



```

C ** MAIN PROGRAM
CALL PEINIT(EPMAX, NMAT, 5, 6, INFO)
CALL GEOMIN(PARINP, NPIP, NM, NB, 7, 6)
N=0
C ** Start a new shower
10 N=N+1
C Set the initial state variables.
CALL LOCATE
CALL CLEANS
C ** Start tracking in the material
20 CALL START
30 CALL JUMP(DSMAX(IBODY), DS)
CALL STEP(DS, DSEF, NCROSS)
IF(MAT.EQ.0) THEN
    GOTO 40 ! Scoring?
ENDIF
IF(NCROSS.GT.0) GOTO 20
CALL KNOCK(DE, ICOL)
C Score relevant quantities
IF(E.GT.EABS(KPAR, MAT)) GOTO 30
40 CONTINUE
C Score relevant quantities
C ** Any secondary left?
CALL SECPAR(LEFT)
IF(LEFT.GT.0) THEN
    GOTO 20 ! Scoring?
ENDIF
IF(N.LT.NTOT) GOTO 10
C Compute averages and write results
END
  
```

□ Variance reduction

When v.r. is useful/needed?

In cases with an intrinsically low probability of scoring contributions to the quantity of interest. This normally results in large statistical uncertainties

Examples: x-ray emission by electrons, small detectors in wide fields, ...

We consider three elementary techniques that are safe (i.e. they keep the simulation results unbiased):

- **particle splitting**,
- **Russian roulette**, and
- **interaction forcing** (except deposited energy spectra)

They are implemented in the subroutine package **PENVARED.F**

A convenient figure of merit to measure the performance of a MC algorithm is the efficiency

$$\epsilon_Q \equiv \left(\frac{\bar{Q}}{\sigma_Q} \right)^2 \frac{1}{T}$$

The time needed to get the rel. uncertainty (σ_Q/\bar{Q}) is $T = \frac{1}{(\sigma_Q/\bar{Q})^2 \epsilon_Q}$

□ PENMAIN. A generic main program

The main program **penmain.f** is designed to solve a wide variety of problems. It operates as a “black box” and is completely controlled through text (ascii) input files. **No programming is required.**

The geometry is described by using the package PENGEO

To define a new problem, we must usually prepare

- the **geometry definition file**
(PENGEO format)
- the corresponding **material-data file**
(by running the program **material**)
- the **input file** containing details on the radiation source, simulation parameters, detectors, variance reduction methods and dose map

By default, **PENMAIN** provides global simulation results such as the energy and angular distributions of particles that emerge from the material system, the average energy deposited in each body, etc.

To generate more specific information, the user can define

❑ **Impact detectors.**

An impact detector consists of a set of active (non-void) bodies, which must have been defined as parts of the geometry.

The output spectrum from an impact detector is the energy distribution of particles that entered any of the active bodies. Optionally, the state variables of all detected particles can be written on a **phase-space file**

❑ **Energy-deposition detectors.**

An energy-deposition detector consists of a set of active bodies; the output spectrum is the distribution of absorbed energy (per shower) in the whole active volume

❑ **A Cartesian mesh for dose tallying.**

□ Structure of the input file

```
.....+.....1.....+.....2.....+.....3.....+.....4.....+.....5.....+.....6.....+.....
TITLE  Title of the job, up to 120 characters.

      >>>>>>> Source definition.
SKPAR  KPARP      [Primary particles: 1=electron, 2=photon, 3=positron]
SENERG SE0        [Initial energy (monoenergetic sources only)]
SPECTR Ei,Pi     [E bin: lower-end and total probability]
SPOSIT SX0,SY0,SZ0 [Coordinates of the source]
SDIREC STHETA,SPHI [Beam axis direction angles, in deg]
SAPERT SALPHA    [Beam aperture, in deg]

      >>>>>>> Input phase-space file (psf).
IPSFN  psf_filename.ext [Input psf name, 20 characters]
IPSPLI NSPLIT        [Splitting number]
EPMAX  EPMAX        [Maximum energy of particles in the psf]

      >>>>>>> Material data and simulation parameters.
NMAT   NMAT          [Number of different materials, .le.10]
SIMPAR M,EABS(1:3,M),C1,C2,WCC,WCR [Sim. parameters for material M]
PFNAME mat_filename.ext [Material definition file, 20 chars]

      >>>>>>> Geometry definition file.
GEOMFN geo_filename.ext [Geometry definition file, 20 chars]
DSMAX  IBODY,DSMAX(IBODY) [IB, maximum step length (cm) in body IB]

.....+.....1.....+.....2.....+.....3.....+.....4.....+.....5.....+.....6.....+.....
```

```

.....+.....1.....+.....2.....+.....3.....+.....4.....+.....5.....+.....6.....+.....
>>>>>>> Interaction forcing.
IFORCE KB,KPAR,ICOL,FORCER,WLOW,WHIG [Interaction forcing]

>>>>>>> Emerging particles. Energy and angular distributions.
NBE EMIN,EMAX,NBE [E-interval and no. of energy bins]
NBTH NBTH [No. of bins for the polar angle THETA]
NBPH NBPH [No. of bins for the azimuthal angle PHI]

>>>>>>> Impact detectors (up to 25 different detectors).
IMPDET EDIL,EDIU,NCHI,IPSF [Energy window, no. of channels and IPSF]
IPSF=+1; particles that enter the detector are transported
as usually. A psf is created.
IPSF=-1; particles that enter the detector are transported
as usually. No psf is created.
IPSF=+2; the simulation of a particle is discontinued when
it enters the detector. A psf is created.
IPSF=-2; the simulation of a particle is discontinued when
it enters the detector. No psf is created.
IDPSF pm_psf_impdet_#.dat [Output psf file name, 20 chars]
IDSPC pm_spc_impdet_#.dat [Output spectrum file name, 20 chars]
IDBODY KB [Active body; one line for each body]
IDKPAR KPAR [Kind of detected particles, one line each]

>>>>>>> Energy-deposition detectors (up to 25).
ENDDDET EDEL,EDEU,NCHE [Energy window and number of channels]
EDSPC pm_spc_enddet_#.dat [Output spectrum file name, 20 chars]
EDBODY KB [Active body; one line for each body]

```

```

.....+.....1.....+.....2.....+.....3.....+.....4.....+.....5.....+.....6.....+.....

```

```

.....+.....1.....+.....2.....+.....3.....+.....4.....+.....5.....+.....6.....+.....
>>>>>>> Dose distribution.
GRIDX  XL,XU          [X coordinates of the enclosure vertices]
GRIDY  YL,YU          [Y coordinates of the enclosure vertices]
GRIDZ  ZL,ZU          [Z coordinates of the enclosure vertices]
GRIDBN  NX,NY,NZ      [Numbers of bins]

>>>>>>> Job properties
RESUME  pm_dumpfile_1.dat [Resume from this dump file, 20 chars]
DUMPTO  pm_dumpfile_2.dat [Generate this dump file, 20 chars]
DUMPP   DUMPP           [Dumping period, in sec]

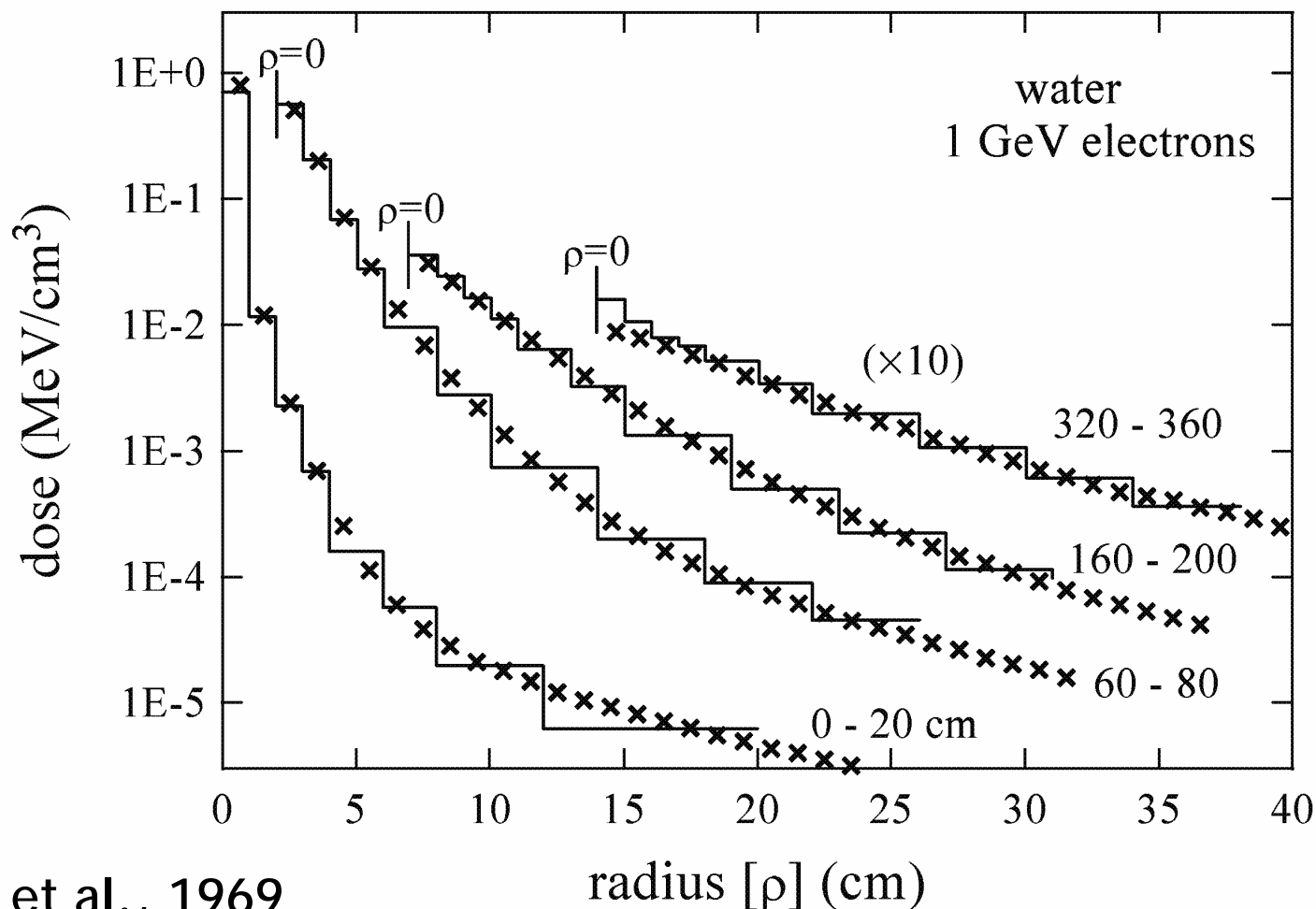
NSIMSH  NTOT          [Desired number of simulated showers]
RSEED   ISEED1,ISEED2 [Seeds of the random number generator]
TIME    TIMEA         [Allotted simulation time, in sec]
.....+.....1.....+.....2.....+.....3.....+.....4.....+.....5.....+.....6.....+.....

```

Examples and applications

A very high energy case

1 GeV electron pencil beam. Radial dose distributions (integrated)

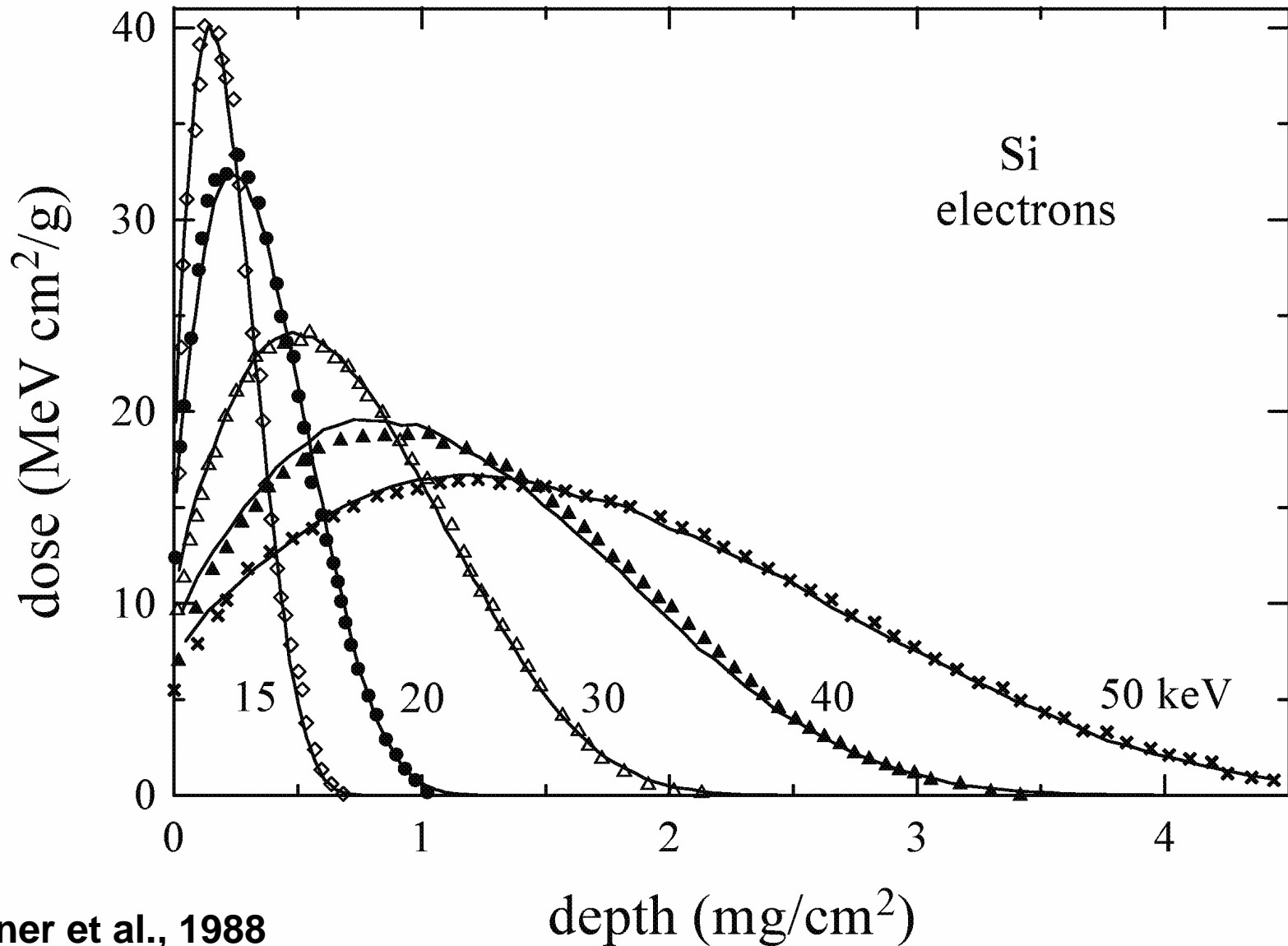


Crannell et al., 1969

CMPWG-II, UF

□ ... and a low-energy case

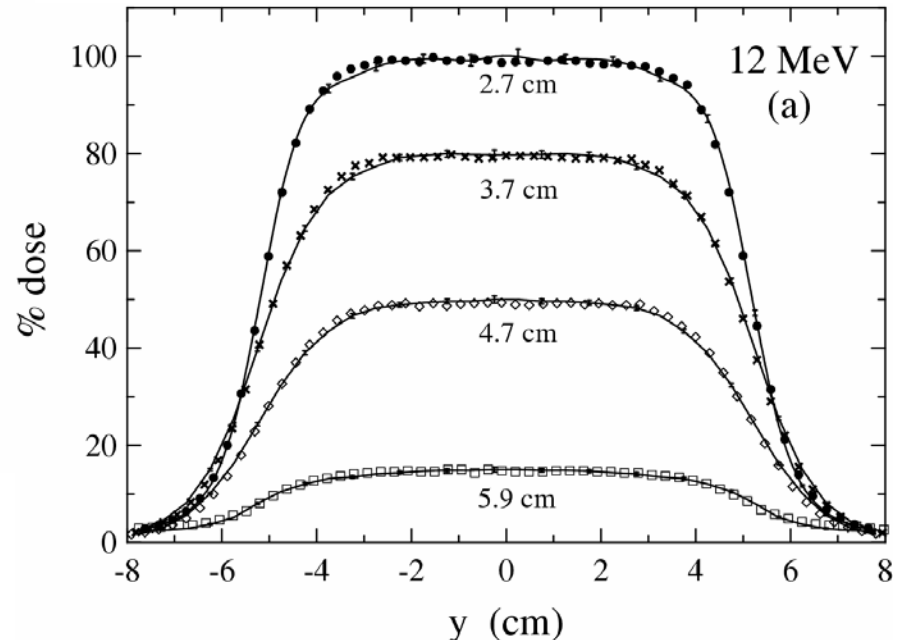
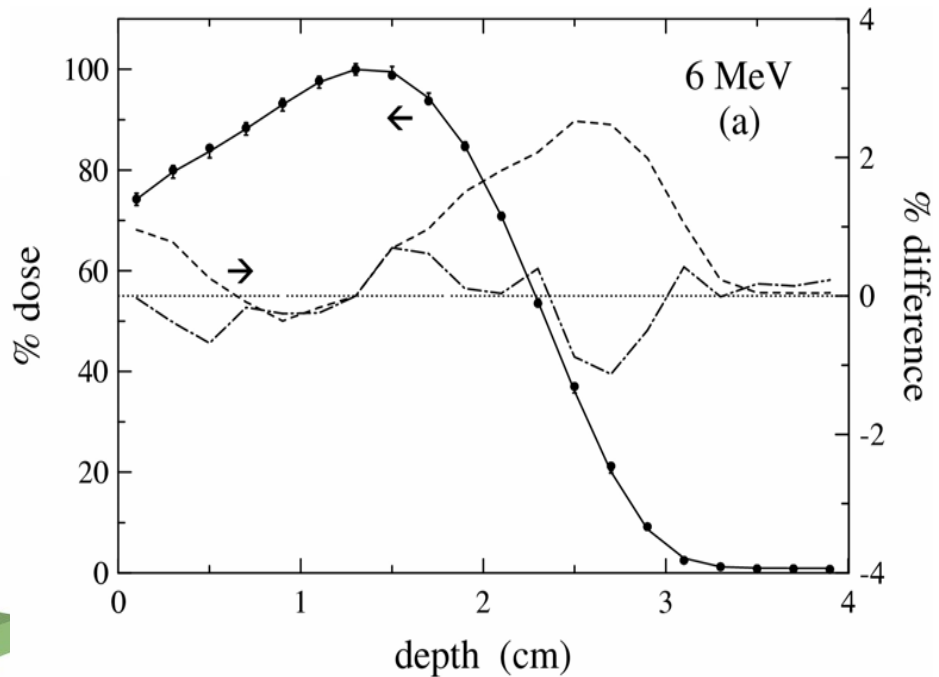
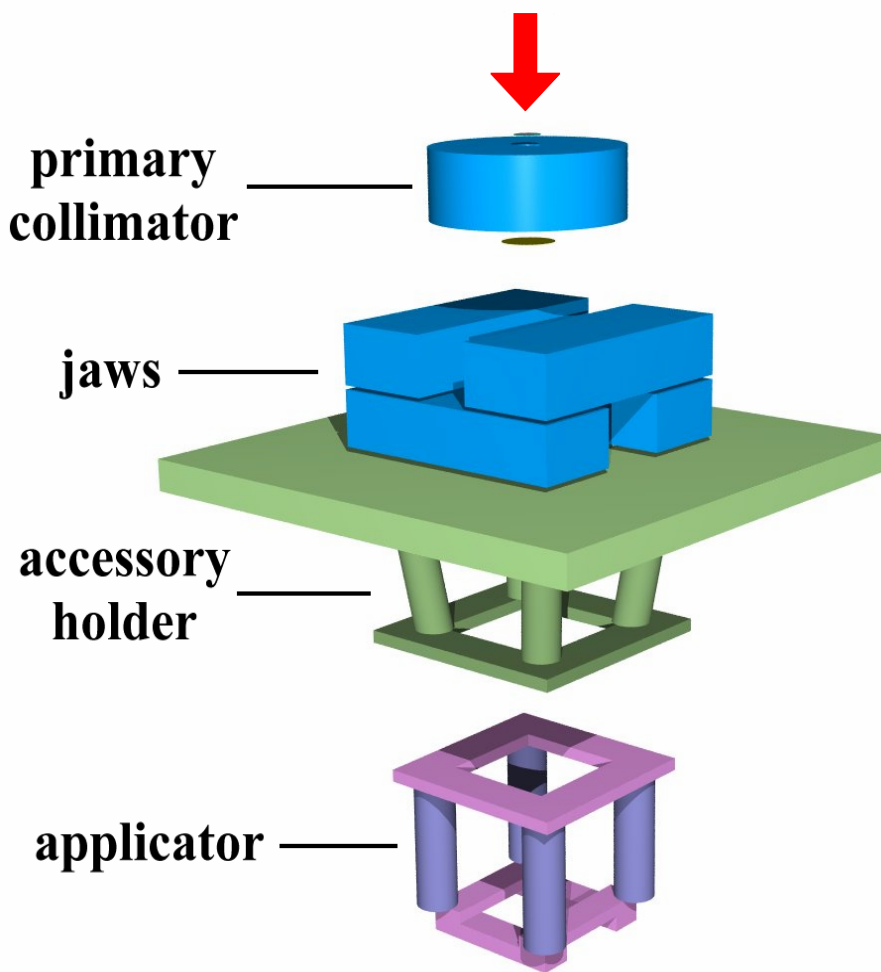
keV electron beams. Depth-dose distributions



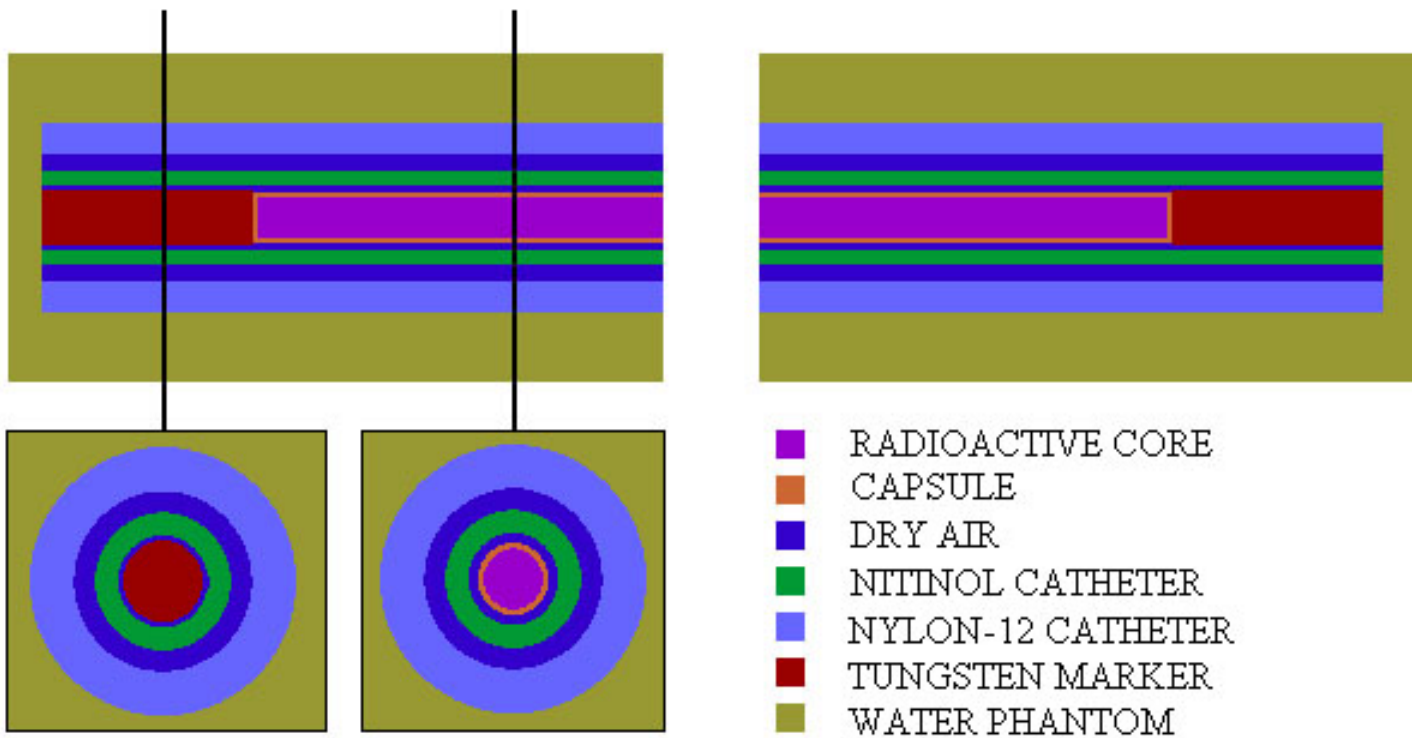
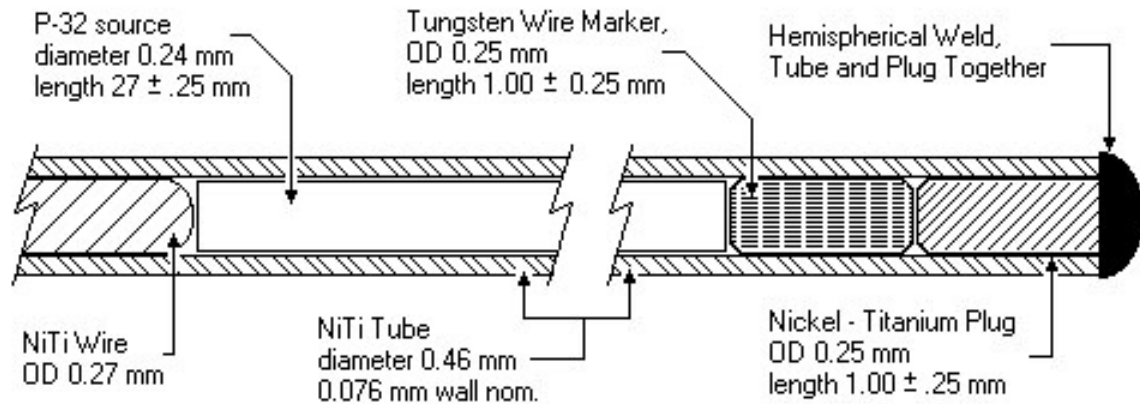
Werner et al., 1988

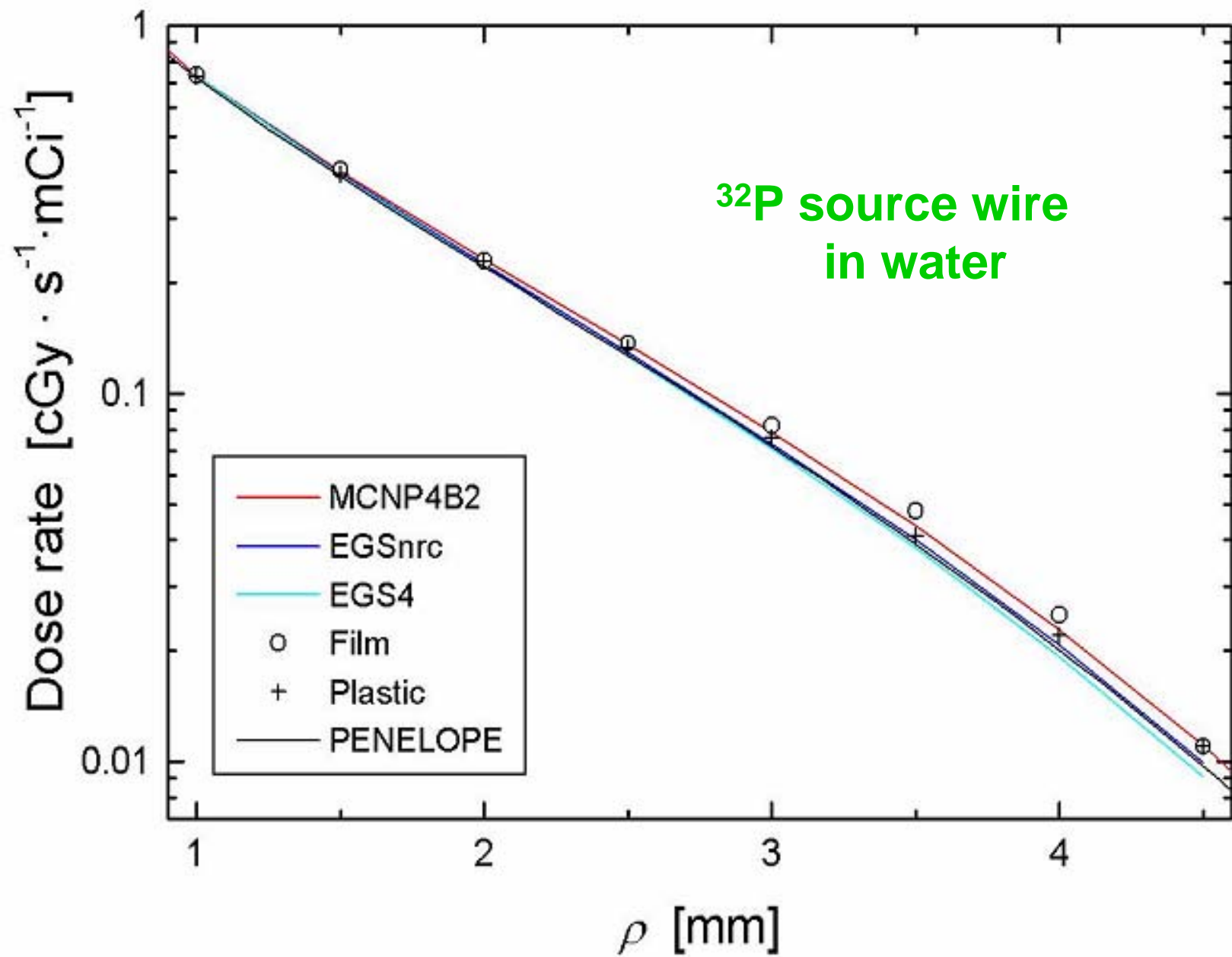
depth (mg/cm²)

Siemens KDS electron accelerator

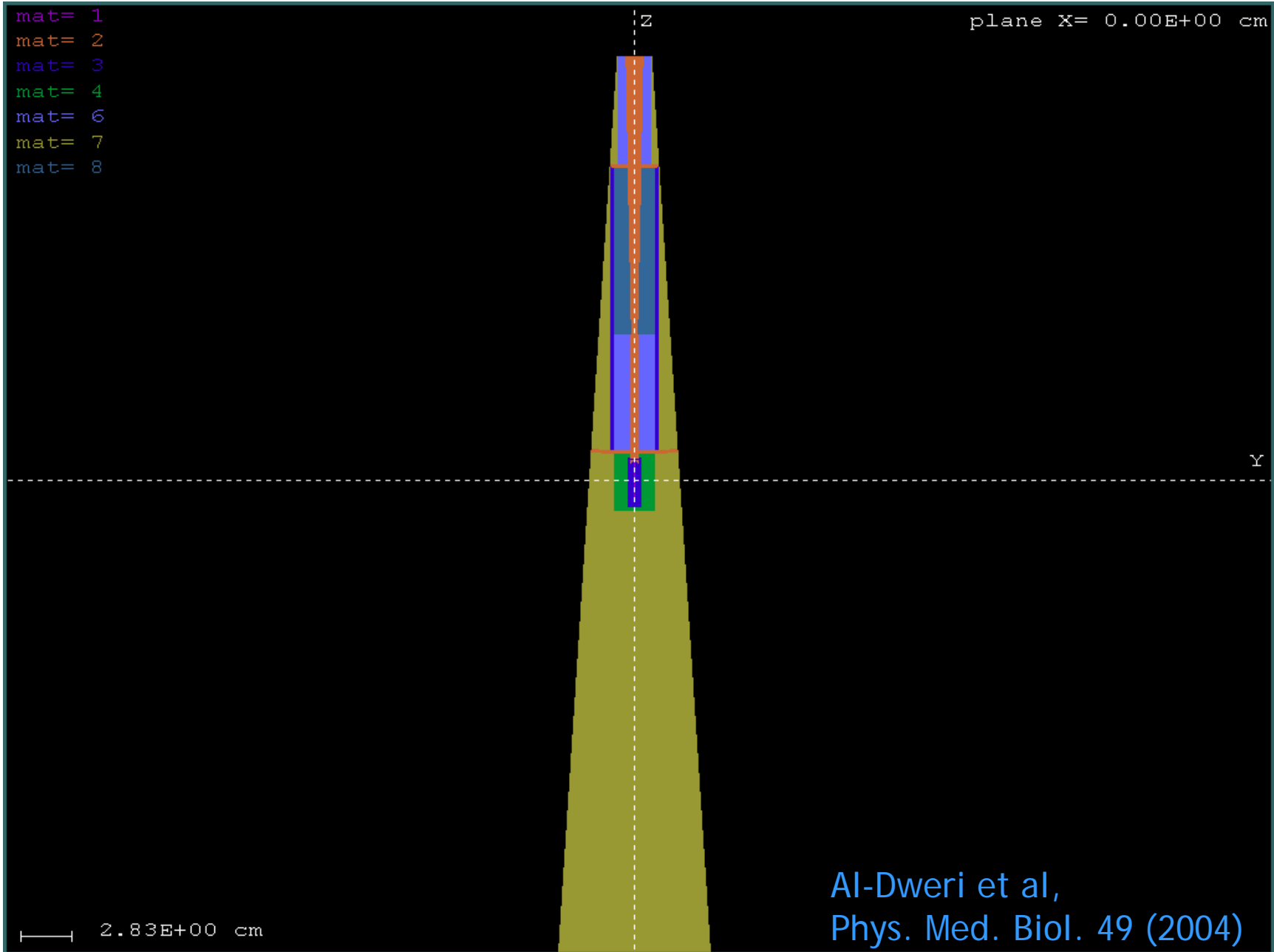


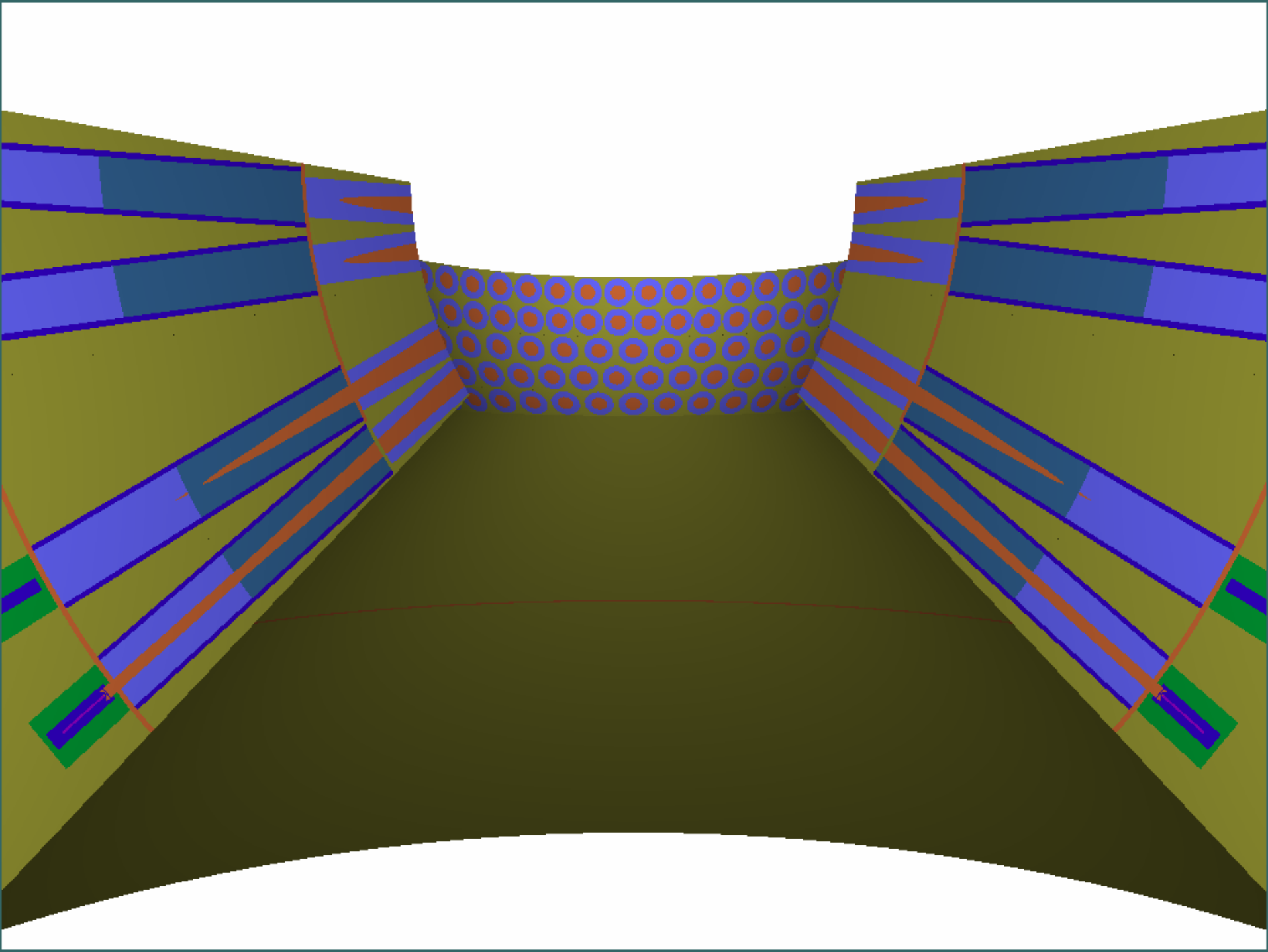
□ ^{32}P source wire for intravascular brachytherapy





Leksell Gamma Knife[®]





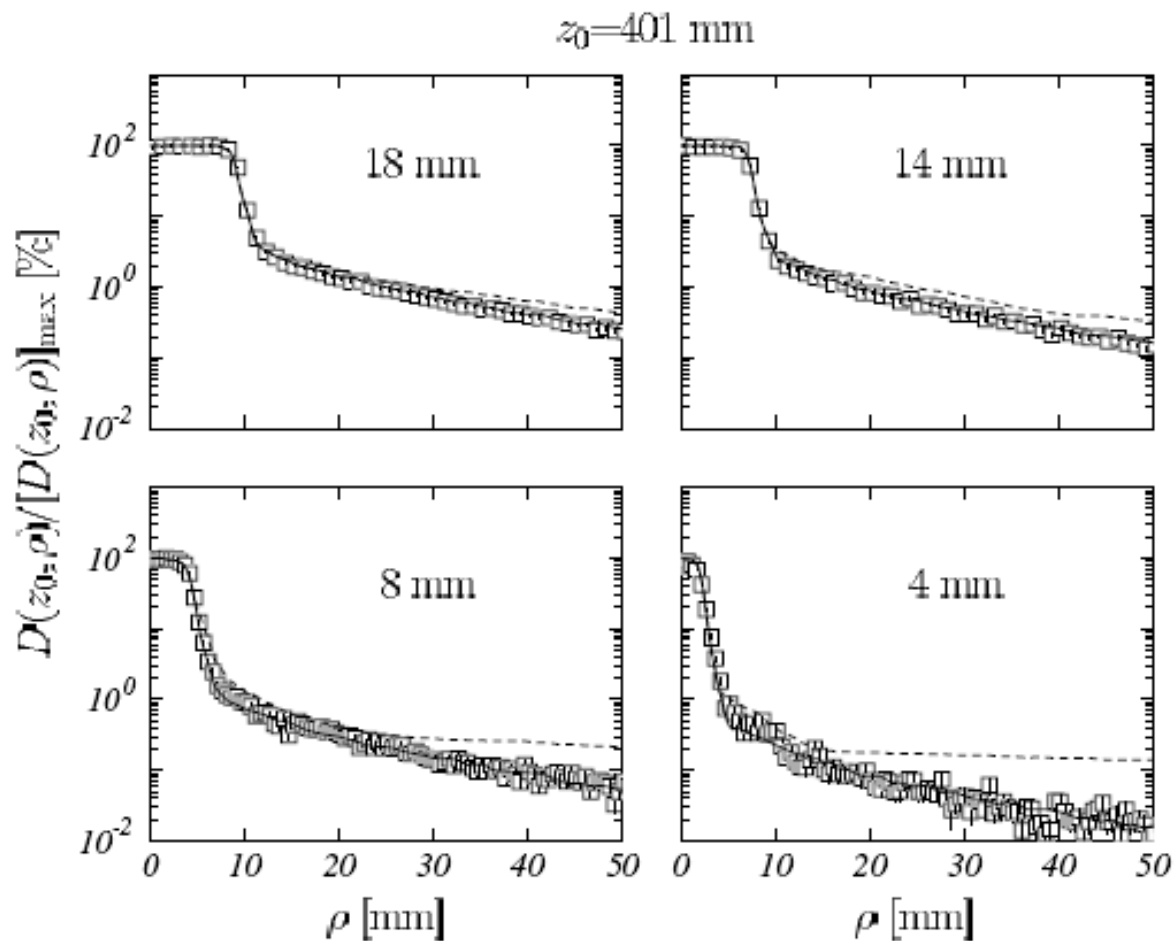
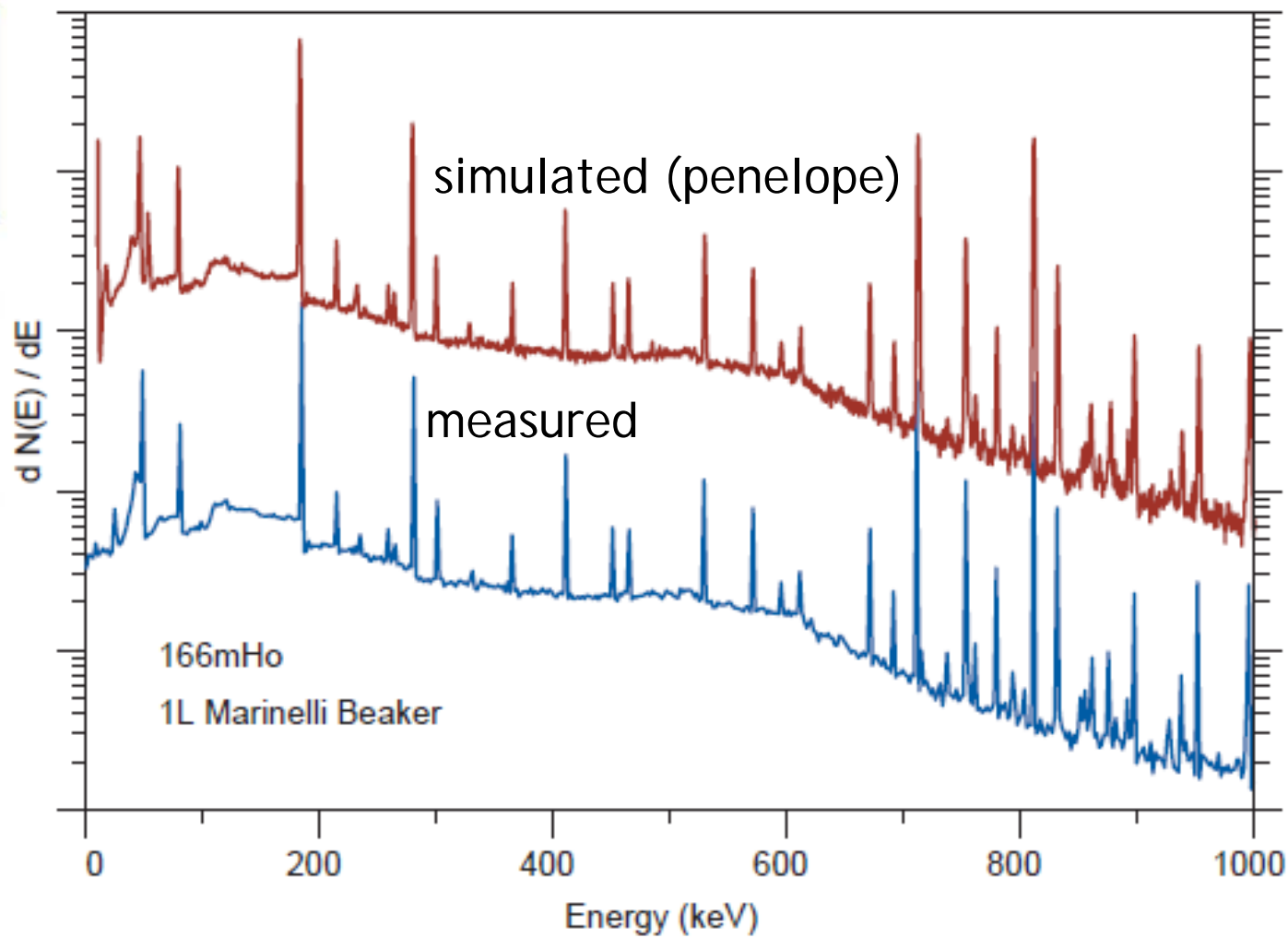
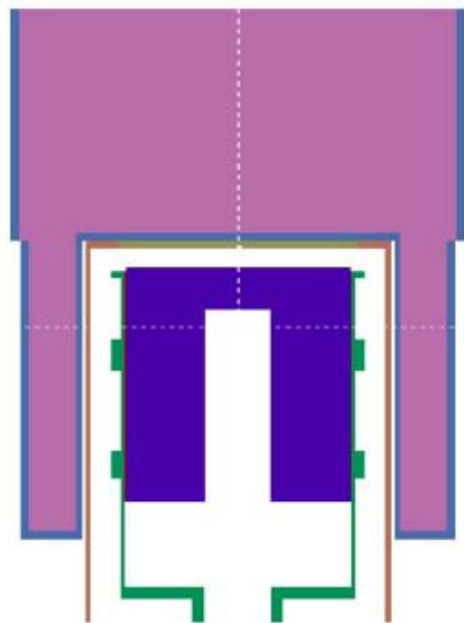


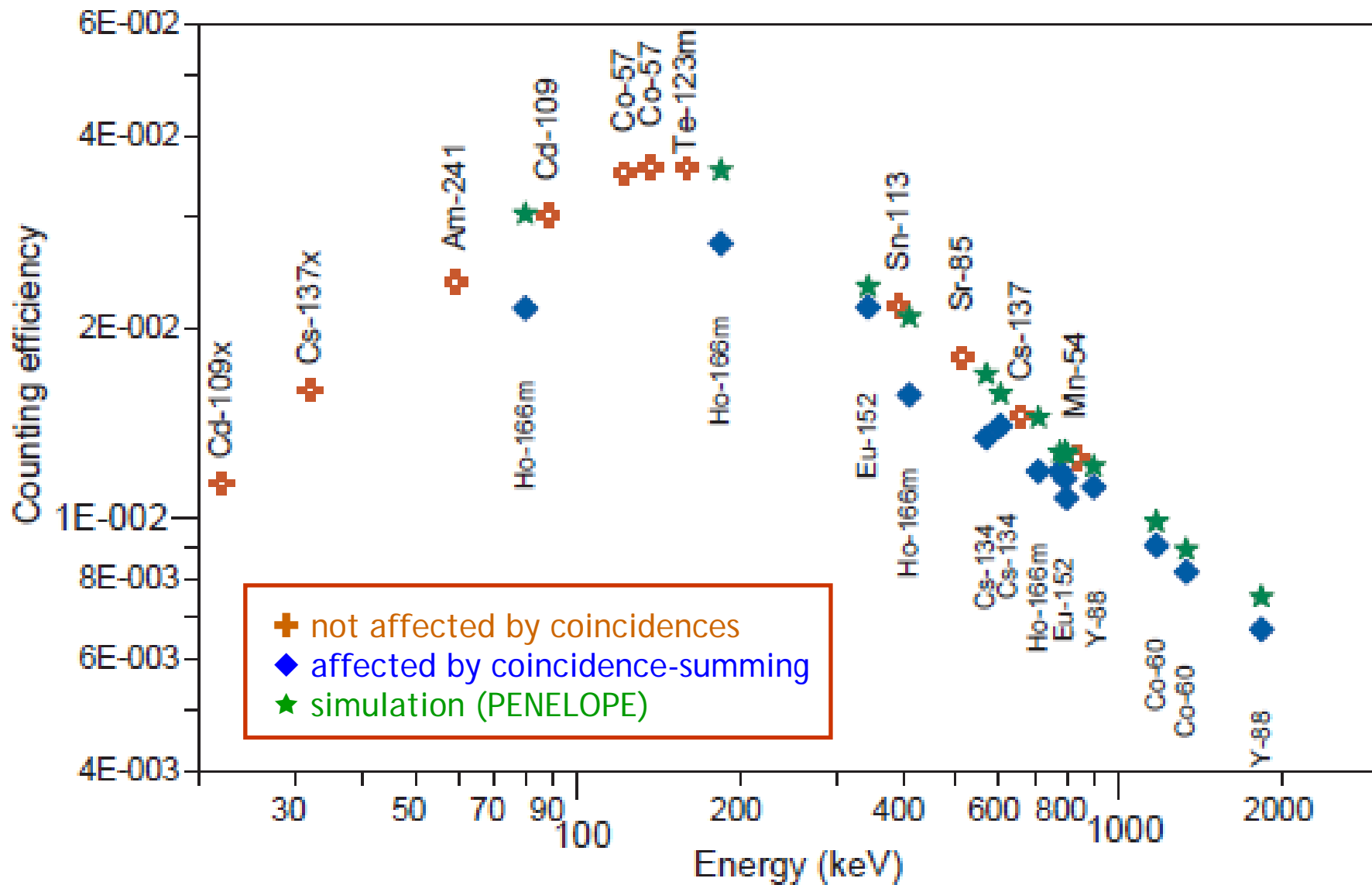
Figure 4. Dose profiles (relative to their maximum) as a function of the radial distance from the beam axis ρ . The results obtained in our simulations at the plane $z_0 = 401$ mm for the four helmets (open squares) are compared with the results of Cheung *et al* (1998) (solid lines) and with the data provided by the manufacturer (broken curves).

Gamma-ray spectrometry

p-type HP Ge detector, Marinelli beaker (García-Toraño, NIMA 2005).



Gamma-ray spectrometry. Detection efficiencies



□ X-ray microanalysis

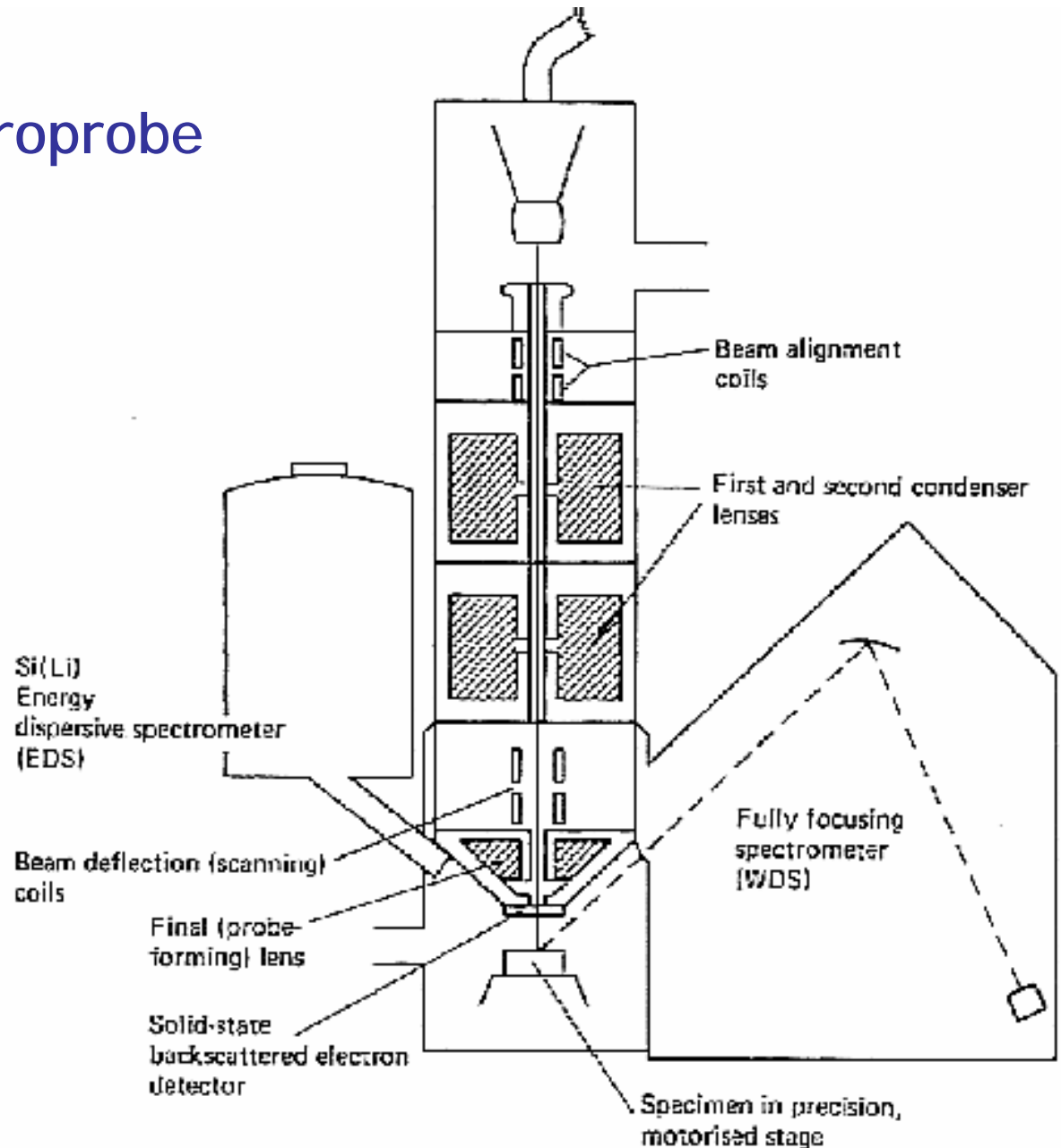
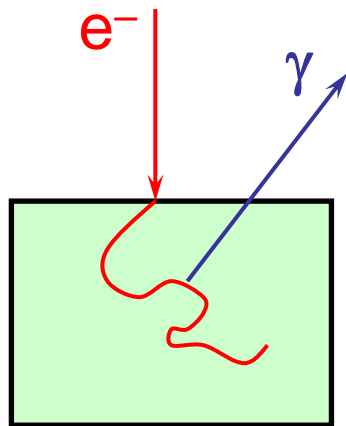
The electron microprobe

$5 \text{ keV} \leq E \leq 45 \text{ keV}$

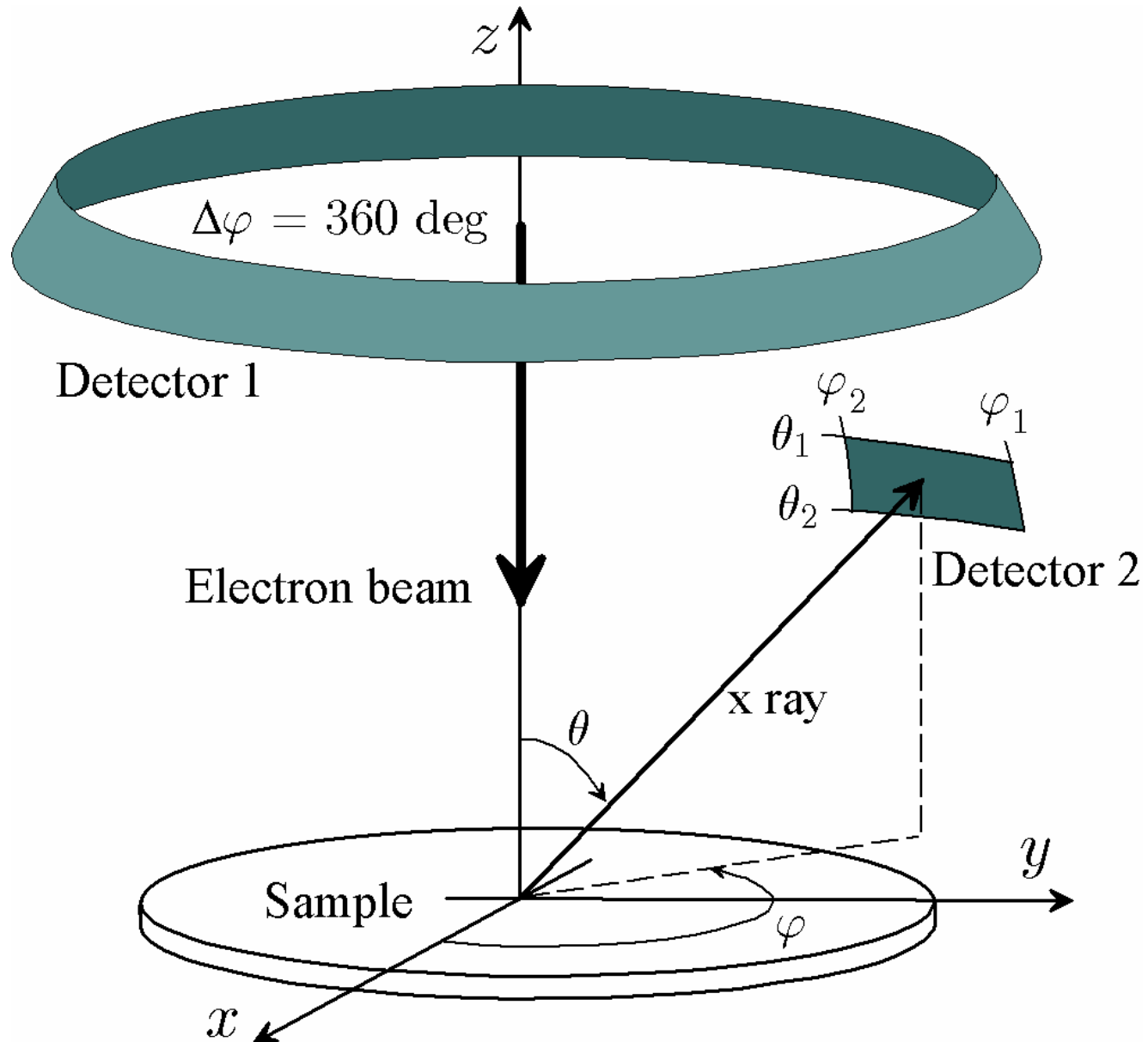
Highly stable

Accurate positioning

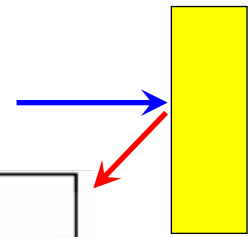
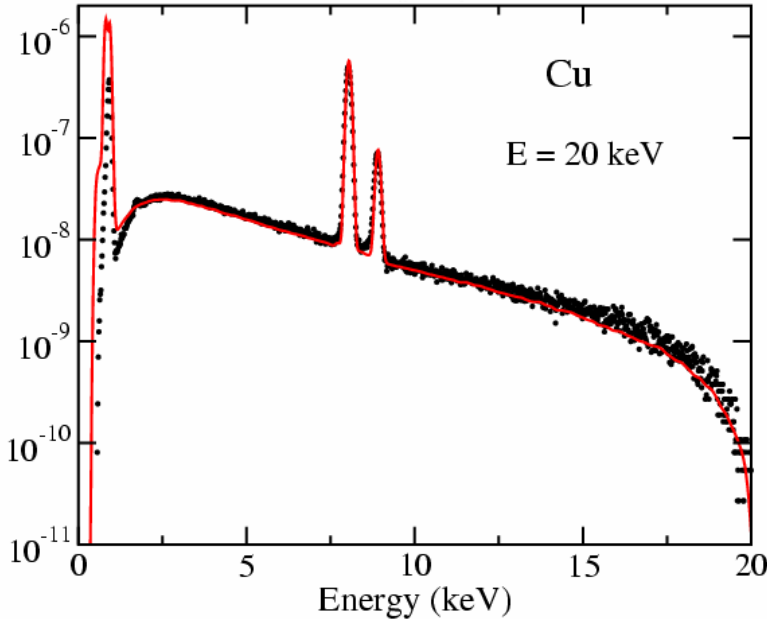
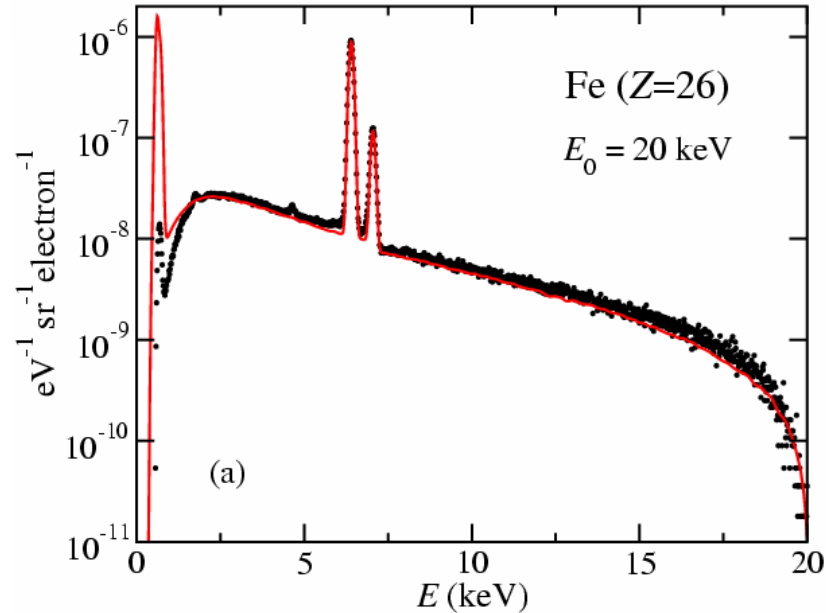
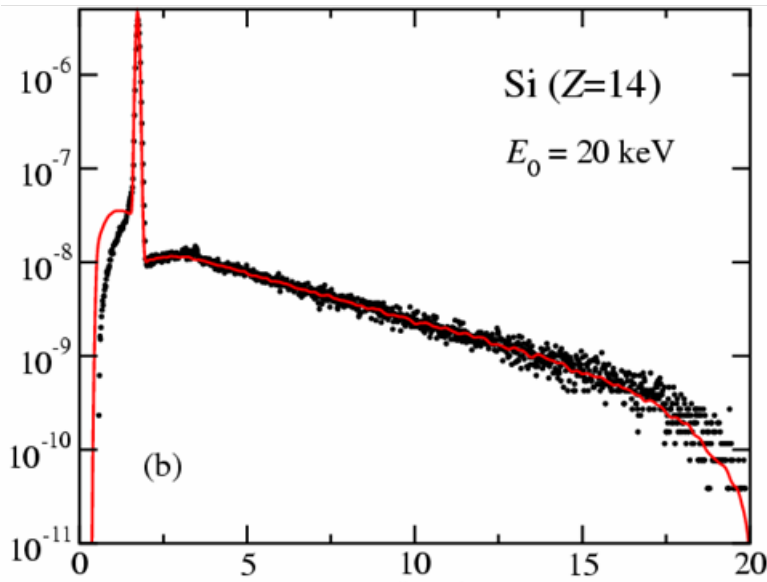
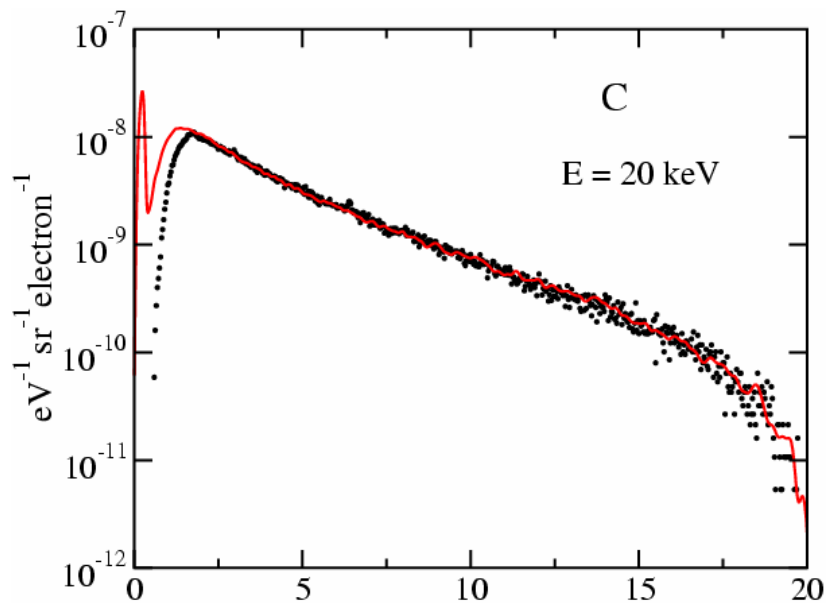
Absolute spectra



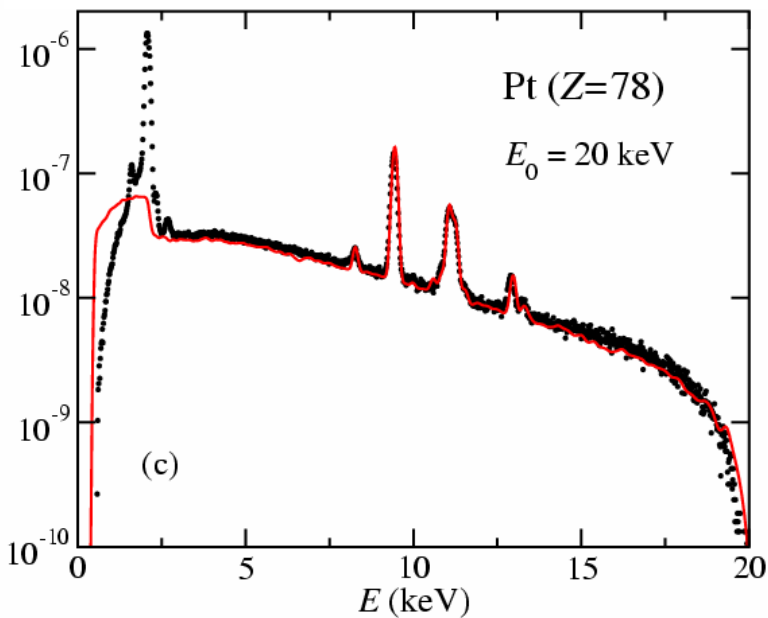
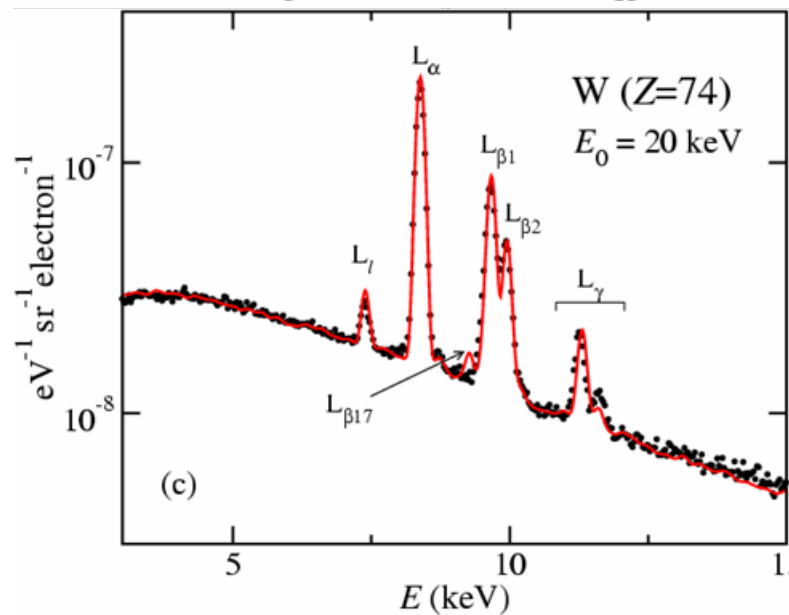
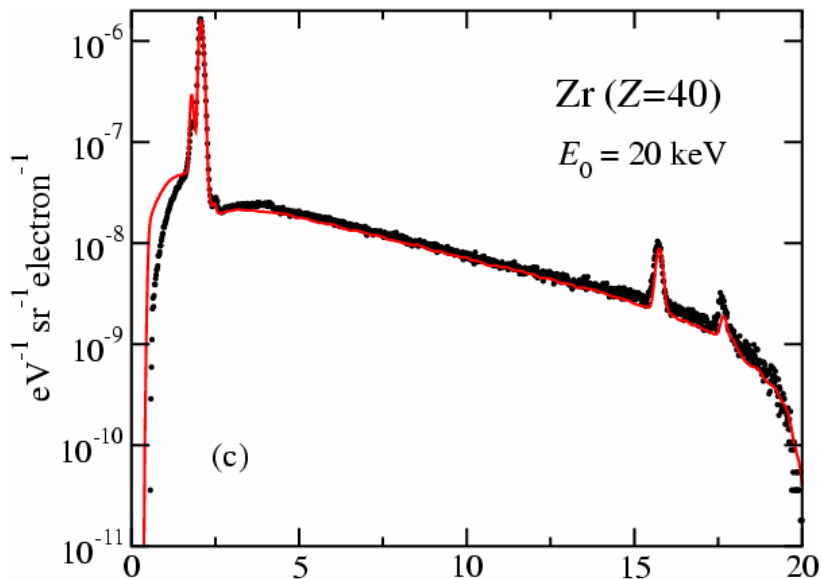
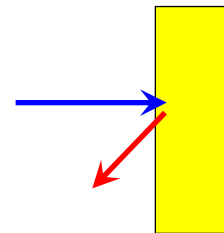
□ X-ray microanalysis. Simulation geometry.



X-ray absolute spectra



X-ray absolute spectra



□ Work in progress

- Inner shell ionization by electron and positron impact
(Distorted-wave Born approximation)
 - Re-evaluation of the density effect on the stopping power
(effective oscillator strengths of individual shells)
 - Photon polarization
 - Adaptive variance reduction (ant-colony method)
 - ... and other practical improvements requested by users
-